



HAL
open science

Contribution of synchrotron radiation to photoactivation studies of biomolecular ions in the gas phase

Alexandre Giuliani, Aleksandar R. Milosavljević, Francis Canon, Laurent Nahon

► To cite this version:

Alexandre Giuliani, Aleksandar R. Milosavljević, Francis Canon, Laurent Nahon. Contribution of synchrotron radiation to photoactivation studies of biomolecular ions in the gas phase. *Mass Spectrometry Reviews*, 2014, The French Regional Issue of Mass Spectrometry Reviews, 33 (6), pp.1-43. 10.1002/mas.21398 . hal-00939803v1

HAL Id: hal-00939803

<https://hal.science/hal-00939803v1>

Submitted on 24 Apr 2023 (v1), last revised 19 May 2023 (v3)

HAL is a multi-disciplinary open access archive for the deposit and dissemination of scientific research documents, whether they are published or not. The documents may come from teaching and research institutions in France or abroad, or from public or private research centers.

L'archive ouverte pluridisciplinaire **HAL**, est destinée au dépôt et à la diffusion de documents scientifiques de niveau recherche, publiés ou non, émanant des établissements d'enseignement et de recherche français ou étrangers, des laboratoires publics ou privés.



Distributed under a Creative Commons Attribution 4.0 International License



HAL
open science

Contribution of synchrotron radiation to photoactivation studies of biomolecular ions in the gas phase

Alexandre Giuliani, Aleksandar Milosavljević, Francis Canon, Laurent Nahon

► To cite this version:

Alexandre Giuliani, Aleksandar Milosavljević, Francis Canon, Laurent Nahon. Contribution of synchrotron radiation to photoactivation studies of biomolecular ions in the gas phase. *Mass Spectrometry Reviews*, 2014, 33 (6), pp.424-441. 10.1002/mas.21398 . hal-04033393

HAL Id: hal-04033393

<https://hal.inrae.fr/hal-04033393>

Submitted on 17 Mar 2023

HAL is a multi-disciplinary open access archive for the deposit and dissemination of scientific research documents, whether they are published or not. The documents may come from teaching and research institutions in France or abroad, or from public or private research centers.

L'archive ouverte pluridisciplinaire **HAL**, est destinée au dépôt et à la diffusion de documents scientifiques de niveau recherche, publiés ou non, émanant des établissements d'enseignement et de recherche français ou étrangers, des laboratoires publics ou privés.



Distributed under a Creative Commons Attribution| 4.0 International License

Contribution of synchrotron radiation to photoactivation studies of biomolecular ions in the gas phase

Alexandre Giuliani^{1,2*}, Aleksandar R. Milosavljević³, Francis Canon⁴, Laurent Nahon¹

¹Synchrotron SOLEIL, L'Orme des Merisiers, Saint Aubin, 91192 Gif-sur-Yvette, France

²UAR1008 CEPIA, INRA, 44316 Nantes, France

³Institute of Physics, University of Belgrade, Pregrevica 118, 11080 Belgrade, Serbia

⁴INRA, UMR1324 Centre des Sciences du Goût et de l'Alimentation, F-21000 Dijon, France

* giuliani@synchrotron-soleil.fr

Running head: Ion activation by synchrotron radiation

Prepared for Mass Spectrometry Review

Abstract

Photon activation of ions in the visible and ultraviolet range attracts a growing interest, partly for its promising applications in tandem mass spectrometry. However, this task is not trivial, as it requires notably high brilliance photon sources. Hence, most of the work in that field has been performed using lasers. Synchrotron radiation is a source continuously tunable over a wide photon energy range and which possesses the necessary characteristics for ion activation. This review focuses on the array of applications of synchrotron radiation in photon activation of ions ranging from near UV to soft X-rays.

Keywords: tandem mass spectrometry; photon activation; synchrotron radiation; ion trap, biomolecules

I. INTRODUCTION

A. Photon-activation and action spectroscopy

The activation of a selected precursor ion is the essence of tandem mass spectrometry (McLafferty, 1980). Several ways exist to increase the ion internal energy and produce fragments, such as inelastic collisions, which is by far the most popular method. However, a more direct activation method is based upon the absorption of a photon by the ionic target. Ion photodissociation goes back to the 1950-1960 period with the very first photodissociation of molecular hydrogen cation see (Dehmelt & Jefferts, 1962) and references therein. In the 1970's, R. C. Dunbar (Dunbar, 1971) has pioneered the field of ion photodissociation in ion cyclotron resonance (ICR) mass spectrometer, reporting the photodissociation of two isolated radical cations produced by electron impact. In

these early experiments an intense Xenon Arc lamp was used in the visible and near ultra-violet with a very large bandpass, as photoactivation requires powerful irradiations.

The appearance of lasers opened new opportunities for this field, as intense source with low divergence were within reach (Cotter 1984). Countless applications have emerged on multiphoton ionization and photodissociation of electrosprayed and MALDI generated ions (Williams & McLafferty, 1990; Guan *et al.*, 1996; Williams *et al.*, 1990; Antoine & Dugourd, 2011; Reilly 2009; Khoury *et al.*, 2002; Madsen *et al.*, 2010). Although lasers are suitable photon sources for ion activation in terms of power and divergence, they are still limited to the visible (vis) and ultraviolet (UV) photon energy range. The pioneering work of Antoine and Dugourd, reviewed recently (Antoine & Dugourd, 2011), using tunable UV-vis laser has brought to light a wealth of information on the lowest electronic excited state of anions. Reilly and coworkers have extensively probed the photofragmentation of protonated peptide ions at two wavelengths in the vacuum ultra-violet (VUV) using excimer lasers (Reilly, 2009). The Brodbelt group has exploited the potential of photodissociation in proteomic analysis (Broadbelt, 2011 and reference therein). The work of the Rizzo group, involving double resonance UV - infrared (IR) experimental scheme, probes photodissociation in a limited UV range to access to infrared properties of specific conformers (Rizzo *et al.*, 2009). This very powerful approach (Nagornova *et al.* 2012) is however out of the scope of this review.

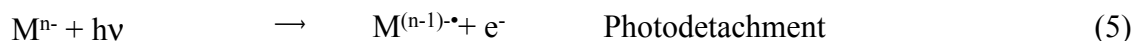
Nevertheless, the possibility to access higher electronic excited state is highly desirable but requires light sources continuously tunable in photon energy and of high brilliance. Third generation synchrotron radiation facilities gather these characteristics but have been used surprisingly only recently for the study of biological ions, although some experimental arrangements were used for decade in atomic ion photoionization. The field of synchrotron radiation based ion activation and spectroscopy of biomolecular ions is in its very infancy, however it appears as an extremely promising and growing trans-disciplinary domain.

B. Synchrotron radiation: from THz to hard X-rays

Synchrotron radiation (SR) is emitted when relativistic charged particles, such as electrons, are accelerated. This quasi-continuous brilliant electromagnetic emission is polarized, and spans a large spectral domain from the THz up to the hard X-rays. SR facilities are composed of an electron gun, electron accelerators (LINAC and boosters) and a storage ring, which maintains the energy and trajectories of the electrons. The emission of the radiation occurs at magnetic devices (bending magnets, undulators or wigglers) placed along the path of the electrons and curving their trajectories. Beamlines are connected to the storage ring and consists of the necessary optics to transfer, filter and shape the synchrotron radiation from the source to the experiment. The particularities of SR, and especially its natural and broad tunability, made it a unique tool in countless domains of science (Helliwell, 1998; Ice *et al.*, 2011; Piancastelli *et al.*, 2010). The primary interactions of electromagnetic radiation with atoms and molecules may be classified into scattering and absorption, the latter being the dominant process in the photon energy range of interest here (Berkowitz, 1979). A typical photoabsorption cross section (df/dE curve) is presented in figure 1 (dashed line) along with a usual spectrum delivered at SR facilities as a function of photon energies

ranging from the infrared to gamma-rays (Hatano, 1999). The positions of typical laboratories light sources are indicated in Figure 1 by vertical arrows. The two shaded parts of the graph represent the regions for which laboratory sources are available apart from synchrotron radiation for photochemistry (vis-UV) and radiation chemistry (hard X-rays and γ -rays). It clearly appears that a large region spanning from the vacuum-UV to soft X-rays is only delivered continuously by SR. Interestingly, the maximum of the photoabsorption cross section (df/dE curve) is found in the exclusive part covered by SR, making this source, as discussed by Hatano (Hatano, 1999), a unique tool filling the gap between photochemistry and radiation chemistry.

The shape of the photoabsorption cross section as a function of the photon energy of gas phase atoms, molecules, and ions is to a large extent very similar to the one presented in figure 1, put aside some specific sharp resonance lines that may appear. However, relaxation processes of the energy deposited into the system by the primary photon absorption may differ strongly depending on the species as for example on the sign of the charged of ions. Some of the major outcomes of photoabsorption may be summarized as follow (Berkowitz, 1979):



Whatever the nature of the target, fluorescence (1) and dissociation (2) processes are possible outcomes following photoabsorption. Photodetachment is however restricted to anions (5), while photoionization is a process in which an electron is emitted from a neutral (3) or cationic target (4), if the photon energy is above its ionization energy (Wang & Wang, 2000). Of course it is possible to observe a combination of these processes such as dissociative photoionization, combining process (3) with the fragmentation of the cation (2).

Visible and UV spectroscopy of biomolecules is routinely performed in the condensed phase; yet, gas phase studies are extremely useful as they provide better control over the target as well as potentially an easier comparison with theoretical calculations. In a general way, the properties of isolated species, such as intramolecular interactions, are accessible in the gas phase without any interference from the solvent, matrix, support or counter ions. It is well known that particular electronic excited states, such as Rydberg's states, are strongly perturbed in the condensed phase (Robin, 1975) and may disappear entirely. Moreover, solution studies are only possible in a restricted wavelength range, owing to the limit of transparency of the containers (cuvettes) or of the solvent itself. In the gas phase, the electronic structure may be probed in a virtually unlimited energy range, bounded only by the available sources, leading to excited states that would not be populated by others means. In comparison to all other spectroscopic techniques, tandem mass spectrometry based methods offer an

additional control on the mass and charge of the sample. This specificity allows systematic studies as a function of the mass and/or the charge states, which are not possible otherwise.

In the following, we will first present a chronological evolution of selected experimental setups for ion activation and spectroscopy that have been associated with UV and soft-X rays beamlines at SR facilities around the world. Photoactivation of multiply protonated ions is then discussed first in terms of the VUV/Soft X-ray spectroscopy and formation onsets, and then in terms of production of fragments generated over the 5 to 20 eV range, in comparison with previous laser- and SR-based experiments and other relevant activation techniques. Finally, we will discuss opportunities regarding photodetachment studies carried out on peptides anions in the 4.5 to 20 eV range.

II. EXPERIMENTAL SETUPS

The use of synchrotron radiation (SR) for the spectroscopy of gaseous atomic and molecular ions is rather challenging from the experimental point of view owing to the limited target ion densities and photon fluxes. Therefore, the classical crossed beam geometry, which is routinely used for spectroscopy of gaseous neutral targets (where a much higher target density can be produced), is not efficient enough and alternative approaches have to be implemented in order to optimize the interaction between the target ions and the photon beam. So far, two different approaches have permitted efficient spectroscopy of gaseous ions. Historically, the first concept to appear, the merged-beam technique, introduced in the 70s (Peart *et al.*, 1973), benefits from an enhanced interaction by literally merging the photon (projectile) and ion (target) beams over an extended length (usually 20-50 cm). In recent years, the use of ion traps emerged as a second approach to perform photoactivation of gaseous ions, bringing new and complementary possibilities with respect to the merged-beam setups. The ion traps setups compensate for the lower ionic current and optical path length by extended irradiation times. Prototypically setups for both merged beam and ion trap experiments are presented in the following sections.

A. Merged beam setups

The merged-beam technique was developed by Peart *et al.*, (Peart *et al.*, 1973) in order to study electron impact processes on atomic ions. It was then adopted by Lyon *et al.*, (Lyon *et al.*, 1986) and implemented at the Synchrotron Radiation Source in Daresbury (UK) for the measurements of photoionization cross sections of gaseous ions. Merged-beam setups have appeared since then at several synchrotron facilities around the world (Covington *et al.*, 2002; Kjeldsen, 2006; Gharaibeh *et al.*, 2011). The field has been reviewed in details by several authors (West, 2001; Kjeldsen, 2006), therefore only a brief description of the basic principles will be given in the present paper. The experimental setup consists on merging the beam of target with a monochromatic photon beam from a synchrotron radiation beamline (see figure 2). Along an extended interaction region, defined by an overlap between the ion and photon beams, photoionization of the primary ion beam can take place. After passing the interaction region, the ion beam containing the precursor ions and the photoionization products is

m/z analyzed by a magnetic device. Both the abundance of the precursor and the photoions are separately measured by a sensitive Faraday cup and a counter device, respectively. The photon beam intensity is also monitored continuously using a calibrated photodiode. Absolute photoionization cross section may then be obtained from the knowledge of the target and the product ion beam current, the photon beam intensity, the efficiency of the particle detectors, the ion and photon beam profiles (measured by using scanning slits), the velocity of the target ions and the known length of the interaction region (Kjeldsen, 2006). Since the ion target densities are rather low (5-6 orders of magnitude lower in comparison to related experiments on gas phase neutral species), the background produced by the photon ionization of the residual gas in the vacuum chamber is particularly important. Therefore, ultra high-vacuum in the interaction region is mandatory. Furthermore, high photon brilliances delivered by undulators are also necessary to those experiments. The accuracy of the cross sections is reported to be typically 10% to 20% (Kjeldsen, 2006), a large part of the error also coming from the uncertainty in the photon flux determination.

Apart from the above-mentioned experimental challenges, another important difficulty of this method lies in the likely large distribution of electronic states of the ionic target. Indeed, when produced typically by using an Electron Cyclotron Resonance Ion Source (ECRIS), the target beam is often composed of a mixture of ions in the ground and metastable states owing to the high temperature of the plasma in the source.

The absolute photoionization cross sections measured by merged beam methods is of great importance to a number of scientific fields, such as plasma science and astrophysics. However, although an impressive amount of photoionization data has been obtained on atoms, (Kjeldsen 2006), little has been reported so far on molecular targets. Hitherto, studies have only been reported on CO^+ (Andersen *et al.*, 2001; Hinojosa *et al.* 2002), and some fullerenes molecules (Scully *et al.*, 2007; Kilcoyne *et al.*, 2010). The difficulty in studying relatively small molecular ions in a merged-beam experiment is that often the doubly charged molecules are not stable with respect to dissociation.

It is also noteworthy that the merged beam arrangement has allowed photoelectron spectra to be measured from ionized calcium atomic ions (Bizau *et al.*, 1991).

B. Ions traps based experiments

Ion traps represent a powerful tool in mass spectrometry. Several efficient trapping concepts have been hitherto developed and have found a broad application as standard mass analyzers, such as Paul traps (March 2009), linear ion traps (Douglas *et al.*, 2004), orbitraps (Perry *et al.*, 2008) and Fourier transform - ion cyclotron resonances (FT-ICR) (Marshall *et al.*, 1998). Ion traps have the particularity to allow performing tandem mass spectrometry at the n -th level, when the following sequence of events is performed:

1. a selected m/z region (the targeted precursor ion) is isolated from the distribution of ions generated in the ionization source
2. the isolated ions in the trap are activated in some way, generating product ions
3. steps 1 and 2 may be repeated for a particular product ion of interest
4. the content of the ion trap is then m/z analyzed

The coupling of an ion trap mass spectrometer with a synchrotron photon beam allows applying a new, complementary, and potentially very efficient activation method, based on resonant absorption of energetic photons (in the VUV or soft X-ray range) by an ion of interest. Moreover, these experimental arrangements also give opportunity to perform a mass spectrometry based action spectroscopy of the trapped ion packet. Therefore, a variety of ionic species with a wide range of sizes and nature can be brought and isolated intact in the gas phase under well-defined conditions. However, although the signal-to-noise ratio can benefit from the prolonged time of ion irradiation (in contrast to the merged-beam experiments), the experimental challenges due to a rather low target density and the limited photon fluxes remain. High-brightness radiation source and improved alignment capabilities that ensure an optimum overlap between the photon beam and the ion packet are mandatory.

The coupling of the ion traps to synchrotron radiation beamlines has been rapidly developing in the last five years. Different traps have been used: FT-ICR for the study of atomic and small molecular organic ions (Thissen *et al.*, 2008), linear ion traps (Hirsch *et al.*, 2009, 2012; Vogel *et al.*, 2012; Niemeyer *et al.*, 2012; Milosavljević *et al.*, 2012a, 2012c; Simon *et al.*, 2010), digital ion traps (McCullough *et al.*, 2009), and Paul traps (Bari *et al.*, 2011; Gonzalez-Magana *et al.*, 2012).

In the following, we will focus on some important experimental developments coupling synchrotron radiation with ion traps technologies. We limit the discussion to the experiments performed in the UV, VUV and soft X-ray ranges with synchrotron radiation only, although a very active community uses routinely ions traps at infrared Free Electron Lasers facilities in France and in Holland (Lemaire *et al.*, 2002; Oomens *et al.*, 2000). We will start by describing the techniques used to study trapped ions formed by electron impact ionization on gaseous samples. Aside their intrinsic interest for atomic and molecular physics, those experiments gave a proof of principle for the use of monochromatic SR in combination with other ion traps. The review will further include a recent, novel experimental setup coupling SR with a radiofrequency ion trap to investigate ion clusters. Finally, we will describe the most recently reported experimental setups that allowed, for the first time, to perform SR spectroscopy of electrosprayed biological ions.

1. *Electron impact ionization*

The coupling of an ion trap with the synchrotron radiation was originally reported in 1991 by Kravis and coworkers (Kravis *et al.*, 1991). In this experiment, performed at the National Synchrotron Light Source facility in Brookhaven (USA), the authors investigated inner-shell photoionization of Ar^{2+} ions stored in a Penning trap. The Ar^{2+} precursor ions were formed by electron-impact ionization of Ar gas in the trap. Precursor ions were then stored and photoionized by a broadband synchrotron radiation beam from a bending magnet. The distribution of photoion charge states following K-shell photoionization of Ar^{2+} ions could be measured. This experimental work has pioneered a new type of study regarding the field of SR-based ion spectroscopy and was of great importance for the further development of the field. Still, its limitations came from the use of the non-monochromatic synchrotron radiation (the so-called white beam), wavelength-resolved spectroscopic study being out of reach at that time.

The feasibility of coupling a FT-ICR ion trap with a soft X-ray beam line, in order to perform wavelength resolved photoionization spectroscopy of Xe^+ precursor relaxed in the pure ground state has been reported in 2008 (Thissen *et al.*, 2008). This experiment, which was performed at the ELETRA light source in Trieste (Italy), has shown that an undulator-based beamline can produce a bright-enough monochromatic photon flux to generate detectable products of the photoionization of ionic species isolated in the trap.

Figure 3 shows a schematic drawing of the open structure of the ICR cell inside a compact permanent magnet FT-ICR mass spectrometer MICRA (Mauclaire *et al.*, 2004). The trapping of the ions inside a 2 cm^3 cell is achieved by the combination of a 1.2 T magnetic field produced by an arrangement of permanent magnet and an electrostatic potential. In order to allow for the light beam through, the Penning trap has been modified and each of the two excitations plates in the original design has been replaced by an open structure. The density of ions in the trap is estimated to be of the order of 10^7 cm^{-3} and the nominal pressure is about 10^{-9} mbar. MICRA possesses a mass resolving power of 73000 at m/z 132 (Mauclaire *et al.*, 2004). Like in the pioneering experiment by Kravis and coworkers (Kravis *et al.*, 1991), the precursor ions were produced by electron impact ionization of the gaseous sample inside the trap. Figure 4 illustrates a typical time sequence of the experiment. The neutral Xe atoms were introduced into the trap by a gas pulse and ionized by 25 eV energy electrons to produce the target ions, which were trapped for about 1000 ms to relax into the ground state before being irradiated by a monochromatic photon beam for 1300 ms. After the irradiation, the mass spectrum was recorded and the procedure was repeated at the next photon energy. The pulsing of the target gas allows one to obtain a high target density, while still keeping a low base pressure in the vacuum chamber limiting the background contribution. The controlled irradiation of the ion packet was achieved by a mechanical photon shutter. Although the signal-to-noise ratio was quite low in this experiment, the authors still managed to obtain relative cross section for the photoionization of Xe^+ ion in the pure ground state.

In contrast to merged beam techniques, ion traps-based experiments can so far only provide relative cross sections, but on cold and relaxed ions. Therefore the combination of these two types of techniques may provide practically complete information regarding the ion spectroscopy (Bizau *et al.*, 2011).

2. Magnetron sputter source

Hirsch and coworkers (Hirsch *et al.*, 2009) have recently reported a novel experimental setup designed to study X-ray and VUV spectroscopy on size-selected clusters in the gas phase by using a quadrupole mass filter and a linear ion trap. The experiment was originally coupled to a soft X-ray beamline at the Berlin synchrotron radiation facility BESSY II (Germany). Clusters of ions were produced by a magnetron sputter source. The setup allowed the authors to measure the ion yield spectra upon X-ray absorption of isolated mass-selected clusters, thereby accessing to fundamental physical properties of transition metal clusters. Figure 5 shows a schematic view of the setup (Hirsch *et al.*, 2009). The clusters were produced with a standard magnetron gas aggregation cluster source, by an evaporation of material from a metal or semiconductor target, induced by argon sputtering. The evaporated material is then carried away from the target by an additional helium buffer gas, introduced radially at the target position. The clusters were

formed by a gas aggregation in a volume cooled down by liquid nitrogen and their size distribution could be tuned by adjusting the helium flow, aggregation length and the pressure. After the exit aperture, the cationic clusters were collected and guided by a radio-frequency (RF) only hexapole ion guide into a quadrupole mass filter. In order to remove as much as possible neutral clusters from the beam, the cluster source exit aperture was tilted with respect to the ion guide. After the selection of a m/z window in the quadrupole mass filter, the clusters ions are transferred into the linear ion trap by ionic lenses and a quadrupole deflector. For an efficient trapping, the helium buffer gas at the pressure of about 10^{-3} mbar is flowed into the trap. The authors also pointed out that because most cluster ions are highly reactive, a high purity helium (99.9999%) buffer gas was mandatory. Additionally, the whole ion trap was cooled down to liquid nitrogen temperature. The authors calculated the maximum cluster ion density in the trap to be about $5 \times 10^8 \text{ cm}^{-3}$. The trapped ion packet was submitted to SR introduced from the opposite side, along the linear quadrupole trap axis. For X-ray absorption spectroscopy, the density of parent ions in the trap was reduced to about $5 \times 10^7 \text{ cm}^{-3}$, which allows for a more efficient trapping of the produced daughter ions. After the photon/cluster interaction, ion bunches are extracted from the trap by applying a pulsed extraction voltage to the exit aperture and transferred by a quadrupole bender into a linear Wiley–McLaren time-of-flight mass spectrometer. Therefore, the experimental system has been designed to perform action spectroscopy, by recording ion yields upon X-ray absorption by the trapped cluster ion precursors. The reported mass resolving power was about $M/\Delta M=300$, which was sufficient for ion yield spectroscopy in the size range of up to 20 atoms per cluster.

The first measurements were performed by coupling the experimental setup to the U49/2-PGM-1 soft X-ray beamline at BESSY II (Germany). The undulator beam line delivered a tunable X-ray beam, which was monochromatized by a plain grating monochromator and focused into the setup via a cylindrical mirror (Hirsch *et al.*, 2009). The testing of the system was performed by measuring the ion yield X-ray absorption spectra of free size-selected pure cobalt cluster ions at the $L_{3,2}$ edge. The most recent work also include the investigation of spin coupling and orbital angular momentum quenching in free iron clusters (Niemeyer *et al.*, 2012), measuring the $2p$ core-level binding energies of size-selected free silicon clusters (Vogel *et al.*, 2012), and also a study of $2p$ X-ray absorption of free transition-metal cations across the $3d$ transition elements (Hirsch *et al.*, 2012).

3. *Electrosprayed ions*

a. Ion trap – ToF instrument

Schlathölter and coworkers have recently developed a hybrid mass spectrometer that allows the coupling of a Paul ion trap with the SR and a time of flight analysis of the ionic products (Bari *et al.*, 2011). The precursor ions were produced by a home-built ESI source. This setup was originally interfaced with a VUV photon beamline of the third generation synchrotron facility BESSY II in Berlin (Germany), in order to study the VUV photoionization and fragmentation of leucine-enkephalin (555.6 Da peptide). Further experiments investigated on size effect on the fragmentation patterns of protonated peptides (Gonzalez-Magaña *et al.*, 2012). Figure 6 presents a schematic of the experimental arrangement (Bari *et al.*, 2011). The protonated ions of biomolecules

are produced by the ESI source, transferred through a capillary, a tube lens, a skimmer and a collisionally focusing quadrupole mass analyzer into the ion trap. The role of the mass analyzer was to select a desired m/z window and to transfer these ions into the Paul trap through its endcap. In order to increase both the efficiency of trapping and of the extraction of the ions through the opposite endcap hole, the helium buffer gas was synchronously introduced by a solenoid pulsed valve up to a pressure of about 10^{-3} mbar. The base pressure inside the trap vacuum chamber was of the order of 10^{-9} mbar. The collisions of the ions with the helium gas damped their motion by reducing their kinetic energy by several eVs and focused the trapped ions to the center of the trap. After the trapped was loaded, a biased skimmer blocked the ion packet and the inlet of the buffer gas was closed, so the pressure in the trap decreased to about 10^{-6} mbar. The trapped ion packet was then submitted to irradiation by the VUV photon beam introduced through a hole in the ring electrode of the Paul trap. The alignment of the setup aimed at placing the focus of the photon beam into the centre of the trap. The period of irradiation was controlled by means of a mechanical shutter, thus the overall photon absorption and intensity of precursor ions dissociations could be adjusted. After the photon beam had been intercepted, both the precursor ions and the products of photon activation were extracted into a time-of-flight (ToF) mass spectrometer by applying a bias voltage to the endcaps of the trap.

The production of the electrosprayed ions, the isolation of a desired precursor species, the trapping of the ions and the detection of the reaction products were spatially separated along the experimental axis, crossed at right angle by the photon beam. The setup proposed by Bari *et al.* (Bari *et al.*, 2011) possesses several features, which are of interest for the photon-spectroscopy of biological ions isolated in the gas phase. The controllable introduction of the helium buffer gas led to low-pressure conditions in the interaction region during the irradiation. Also, the use of a TOF spectrometer may allow for theoretically unlimited m/z range ion analysis. On the other hand, a linear arrangement of the ESI source and the ion optics may cause a significant background contribution of neutral molecules from the ESI source present in the trap during the irradiation. Even with the best alignment between the mass spectrometer and the photon beam, the maximum interaction region is defined by the overlap between the spherical ion packet in the centre of the Paul trap and the photons beam crossing it at the focal point. The reported mass resolving power of about 200 may not be sufficient to unambiguously identify the charge state of heavier and multiply charged fragment.

b. Linear ion trap

Our group has developed an experimental setup that can be easily coupled to synchrotron beamlines. The objectives were both to develop a new and complementary tandem mass spectrometry technique based on either VUV or soft X-ray activations and to access physical properties of intact large biological ions in the gas phase. The experimental arrangement (Milosavljević *et al.*, 2011, 2012c) is based upon a commercial linear quadrupole ion trap mass spectrometer (“Thermo scientific LTQ XL”), equipped with ESI and nano ESI probes, which offers several advantages, as discussed below.

The commercially available ESI source of the LTQ XL sprayed ions under an angle of 45° , which, together with a slightly displaced transfer tube, significantly reduced the background from the neutrals. The electrosprayed ions were introduced into

the so-called two-dimensional (2-D) quadrupole ion trap (Schwartz *et al.*, 2002) after passing through the capillary transfer, the tube lens and a system of multipole lenses. The quadrupole consisted of rods with a hyperbolic profile, and each rod was cut into three axial sections of 12, 37, and 12 mm length (Schwartz *et al.*, 2002). The ion trapping was achieved by a combination of DC and RF fields applied to each rod. Additionally, the helium gas was introduced directly into the trap at the pressure of 10^{-3} mbar. As explained earlier, the collisions with helium cool down the ions and improve the trapping efficiency. The ion ejection was made through 0.25mm height slots that had been cut along the middle side electrodes (Schwartz *et al.*, 2002). The ejected ions were detected by conversion dynodes. The perpendicular ion ejection with respect to the axis of the ion guiding was crucial for the present setup because it allowed an easy introduction of the photon beam directly into the trap through the existing hole in the back lens. Therefore, the coupling to a beamline could be performed in an elegant way and without the need of changing the original trap design (e.g. by piercing holes), which could have imparted on its performance. Moreover, the linear geometry of the 2-D trap, forming a quasi-cylindrical ion packet, allowed for an extended overlap with the photon beam in comparison with the 3-D trap. Additionally, the introduction of the photon beam from the back side of the trap made possible a fine pre-alignment of the position of the trap by detecting from the front side the visible photon beam passing through the spectrometer along the axis of the ion guiding lenses. An optimal alignment between the photon beam and the ion packet was crucial to achieve a high signal-to-noise ratio. LTQ mass spectrometers appear as very versatile, robust and highly performing instruments with a maximum mass resolving power above 25000, when compared to others for proteomic analysis (Thelen & Miernyk, 2012).

Figure 7 presents a schematic of the original coupling of the linear ion trap with the DESIRS beamline (Nahon *et al.*, 2012) at the SOLEIL synchrotron radiation facility, Saint Aubin (France) (Milosavljević *et al.*, 2012c). The VUV photon beam was produced by the electromagnetic undulator OPHELIE 2 (giving a 7% bandwidth), which was further monochromatized by a 6-meter normal-incidence monochromator (NIM). In order to obtain a high spectral purity of the incident photon beam, which was of a crucial importance for the spectroscopic and moreover fragmentation applications, the gas filter of the beamline was used to remove the harmonic content of the source spectrum, thereby ensuring spectral purity. Additional filtering at very low energies was performed with MgF₂ and suprasil windows inserted on the optical path. Downstream the NIM, the beam was deflected and refocused into the ion trap setup, which was mounted on one of the post-focusing arm port. A beam shutter (Milosavljević *et al.*, 2012b) was used to let the incoming VUV light go inside the trap for a controlled period of time. The shutter was made of a vacuum-compatible electro-motor (Kuhnke) and achieved short (about 1 ms), and reproducible chopping times under high-vacuum conditions and with a good reliability during all the experimental time. The sequence of events to record a photon activation tandem mass spectrum of a selected ionic precursor and at a given photon energy was as follows:

1. the electrosprayed ions were injected and stored in the trap;
2. a desired precursor (m/z window) was selected and isolated in the trap (by ejecting all other ions);
3. when a desired precursor ion capacity was reached, the beam shutter opened, thus starting the irradiation;

4. after the desired time of irradiation, the shutter intercepted the beam;
5. the mass spectrum was recorded.

Because of the low target density and the limited photon flux, as discussed earlier, SR photoactivation of the trapped ions in the gas phase is only possible if a perfect alignment between the ion packet and the photon beam is achieved. Note that in the case of LTQ XL mass spectrometers the ion packet is approximately a cylinder of 2 mm diameter and 20 mm length. Therefore, great care had to be taken to ensure easy and repeatable alignment of both ion and photon beams. For this purpose, the mass spectrometer itself had to be aligned on a fixed photon beam, in contrast to the situation encountered when dealing with laboratory sources. Thus the supporting frame of the LTQ was made of five different plates, so the mass spectrometer that was mounted on the top of the system could be positioned with respect to four independent motions: 3-axis of translations and a rotation around the vertical axis passing through the center of the cylindrical trapping region, to obtain co-linear beams. The focus of the photon beam was set approximately at the position of the photon shutter, optimizing both the operation of the shutter with a tight focus, and the transverse overlap with the ion packet. Finally, a vacuum manifold with a turbo pumping stage had been placed between the mass spectrometer and the beamline to accommodate for the pressure difference between the beamline post-focusing arm (10^{-8} mbar) and the LTQ (10^{-5} mbar).

III. PHOTOACTIVATION OF PROTONATED IONS

A. Photoionization threshold

Photon irradiation of a protonated molecule $[M+nH]^{n+}$ may lead to emission of a photoelectron and formation of a radical cation in a photoionization event. Monitoring the abundance of the radical $[M+nH]^{(n+1)+\bullet}$ as a function of the photon energy allowed measuring the ionization threshold for the $[M+nH]^{n+}$ precursor ion. The case of valence shell and inner-shell ionization are discussed separately in the following.

1. Valence shell

a. Pioneering electron impact studies

In the beginning of the 2000s, pioneering experiments have been reported in which electrosprayed ions from poly-peptides below 3500 Da were submitted to electron impact ionization in FT-ICR traps (Budnik *et al.*; 2002, Budnik *et al.*, 2000). These authors have reported the first study on charge-state resolved electron impact measurement of the ionization energy for several peptides and small proteins (Substance P, [Arg-8]-vasopressin, rennin, insulin B-chain and melitin). They observed an increase of the ionization threshold for a given species as its charge state was increased. It appeared that, for polypeptides in the 1 to 3.5 kDa mass range, the ionization energy values varied linearly with the charge state. In this model, the slope of 1.1 eV per charge accounted for the increasing attractive Coulombic interaction between the departing electron and the ion core as the charge increases, resulting in an enhancement of the

ionization energy. The intercept of 9.8 eV represented the ionization energy of a hypothetical neutral peptide. It is worth emphasizing here that measurements of the ionization energy are still lacking for several amino acids (Close, 2011). The authors have compared their finding to an average value of 8.4 eV for the adiabatic IE of amino acids, but without discussion of the nature of the molecular orbital.

b. VUV photoionization studies

Photoionization measurements at the DESIRS beamline at SOLEIL using the setup described in II.B.3.2 were performed on cytochrome C, ubiquitin, bovine pancreatic trypsin inhibitor (BPTI) (Giuliani *et al.*, 2012), and substance P and are presented in figure 8 together with the previous electron impact data (Budnik *et al.*, 2002). For substance P, the two kinds of measurements agree satisfactorily well, although for $z = 1$ the Ionization Energy (IE) measured by photoionization appeared slightly lower than the one from electron impact. The 11.0 ± 0.4 eV reported for singly protonated substance P is a combination of MALDI and ESI measurement. However, the ESI data gave a 10.6 ± 0.5 eV, which is consistent with our 10.3 ± 0.1 eV. The ionization energies are obtained with less than 1.5 % accuracy by photon impact, much better than the 4 to 6 % from electron impact.

For VUV IE measurements of peptides and proteins larger than 3.5 kDa (ubiquitin, bovine pancreatic trypsin inhibitor, and for cytochrome C), a quasi-linear trend over all charge states was observed for BPTI (green full circles, figure 8) in line with the earlier reports on peptides, but this was apparently not true for cytochrome C (orange full squares, figure 8) and ubiquitin (red full triangles, figure 8). Indeed, for the latter proteins, the ionization energies increased for the two lowest charge states and then got stabilized for several charge states. According to the model of Budnik and coworkers (Budnik *et al.*, 2002), the ionization energies were expected to increase by 2.2-3.3 eV between charge state 5 and 7-8 for cytochrome C and ubiquitin. For charge state larger than +8, the ionization energies values increased again with z but with a much lower slope than expected from the linear model. The charge state region where both ubiquitin and cytochrome C ceased to exhibit a linear increase of the IE with z had been suggested to correspond to the regions where the proteins unfolds, as evidenced by ion mobility mass spectrometry (Shelimov *et al.*, 1997; Shvartsburg *et al.*, 2006; Badman *et al.*, 2005; Clemmer *et al.*, 1995; Valentine *et al.*, 1997). BPTI differs from the other two studied proteins by the presence of three disulfide bridges, which provide it with a more constrained structure, preventing important unfolding. Thus the ionization energies measured as a function of the charge state have appeared to correlate with the gas phase structure of proteins, and more precisely to their ternary structure. The initial modeling for the charge-state dependence of ionization energy (Budnik *et al.*, 2002) only took into account the electron-ion Coulomb interaction. A correction to that model has been proposed (Giuliani *et al.*, 2012) in which the ionization energy of the neutral species (E_I^0) was complemented by an energetic terms that described the cost of removing the photoelectron from a spherical potential created by the proteins with z protons: $E_I(z) = E_I^0 + ze^2 / 4\pi\epsilon R_e(z)$, where $R_e(z)$ is the mean electrostatic radius of the protein cation, ϵ is the absolute permittivity of the medium and e the electric charge. This model establishes a univocal correspondence between the ionization energy measured for charge state z and a mean electrostatic radius $R_e(z)$ created by the z charges on the proteins. Knowledge of one parameter (E_I or R_e) allows the

determination of the other. From molecular dynamic calculation of population of radii of gyration for each charge state, the evolution of the ionization energy curve as a function of the charge state could be reproduced. Conversely, the ionization curve could be used to calculate the mean electrostatic radii, providing that the ionization energy for the neutral species is known. For cytochrome C, E_I^0 was taken equal to the ionization energy of tryptophane (Gaie-Levrel *et al.*, 2011), the amino acid with the lowest ionization energy found on the protein (Close 2011, Kalcic *et al.*, 2012). The mean radii extracted by this method are compared to ion mobility cross section from the literature (Shelimov *et al.*, 1997) in figure 9. The agreement between the two sets of measurement is excellent, as the mean radii increase for z values where extended conformation appear. Both curve exhibit very parallel shape. It is worthy noting, that the cytochrome C solutions electrosprayed for the photoionization measurements (Giuliani *et al.*, 2012) were prepared in the same manner as those used for ion mobility measurements (Shelimov *et al.*, 1997). A striking feature is the correspondence between the mean electrostatic radii and the experimental radii of gyration measured by SAXS either in solution (Akiyama *et al.*, 2002; Kamatari *et al.*, 1996) or on stored ions in a digital ion trap (McCullough *et al.*, 2009). More work is needed here to establish whether this agreement is fortuitous or not. Nevertheless, this work has provided a powerful mean to extract geometrical parameters for gas phase ions from measurements of their ionization energies. This work also suggests that the highest occupied molecular orbital (HOMO) should be found on the amino acids with the lowest IE. When aromatic amino acids are present, the HOMO is very likely located on their side chains. Moreover, it is clear that the ionization energy should be considered as a quantity averaged over the populations of conformers and charge states and not as a defined and fixed number.

2. Inner-shell

Inner-shell excitations differ from valence excitations in the probed molecular orbitals. Soft X-rays have enough energy to excite the core electrons localized around the atoms. When dealing with second row elements, the transitions involve 1s electrons located on specific atoms such as carbon, nitrogen or oxygen. Upon photoabsorption below the ionization threshold, these core electrons are promoted to unoccupied bound states. The resulting positive hole may decays via resonant Auger or X-ray fluorescence. Above the ionization threshold, the core electron is ejected into the ionization continuum, and the dominant relaxation process is normal Auger decay (Piancastelli *et al.*, 2010). Auger ionization thus results in the production of doubly ionized species. Consequently, monitoring the relative cross section for the production of a given ionized species (or a specific fragment ion) upon inner-shell photo-excitation of a molecule directly gives insight into a site-specific excitation and relaxation process.

C, N and O near-edge ion yield spectroscopy of 8+ cations of cytochrome C has been measured (Milosavljević *et al.*, 2012a) by coupling a LTQ XL linear ion trap with the soft X-ray beamline PLEIADES at the SOLEIL synchrotron radiation facility. Figure 10 reproduces the ion yields obtained at the carbon (280 - 302 eV), nitrogen (392 - 413 eV) and oxygen (527-544 eV) edges. The partial ion yields extracted showed significantly different behaviors for single and double ionization channels, which had been qualitatively explained by different Auger decay mechanisms. The single

ionization yields agreed very well with existing near-edge X-ray absorption fine structure (NEXAFS) spectra from thin films of peptides and proteins (Stewart-Ornstein *et al.*, 20007). However, the shape of the C-edge yield was found to differ from previous gas and condensed phase measurements, but the position of the peaks was found in excellent agreement with those studies. The sharp features A and B observed in figure 10(a) have been assigned to C 1s $\rightarrow \pi^*$ transitions involving the aromatic amino acids and the carbonyl group, respectively, in agreement with literature data on condensed proteins and gas phase amino acids (Stewart-Ornstein *et al.*, 2007). The broad contribution at 293 eV corresponded to several overlapping σ^* resonances. For the N and O edges, transitions $1s \rightarrow \pi^*_{amide}$ were also observed at the expected energies (features D and F). Feature E in figure 10(b) has been proposed to be associated with the $\sigma^*(C-N)$ resonance, still in excellent agreement with the NEXAFS literature.

Thus, this work has opened up new opportunities for near-edge X-ray spectroscopy of biological macromolecules in the gas phase, as a complementary technique to NEXAFS performed on thin organic films and liquids. Indeed, condensed phase experiment suffers from serious radiation damage issues, as well as surface, intermolecular, and solvent effects, which is obviously not the case in gas phase experiments.

B. Photo-fragmentation of peptides and proteins cations

Ultra-violet absorption of polypeptides has been extensively studied in the condensed phase, mainly in the field of circular dichroism for the characterization of molecular conformations. Specific difficulties in the study of the electronic structure of biological species pertain to the nature of the targets. Indeed these molecules contain a variety of chromophores and are of low symmetry. They are of high molecular weight and of low vapor pressure, making their production in the gas phase very challenging as neutral, which explains why their study has been so far mainly limited to the liquid phase. However, photoabsorption of polypeptides may be viewed to a first approximation as the superposition of individual spectra arising from the constituting chromophores. Three main groups have been found to contribute: aromatic amino acids and histidine, the peptide bond and the side chains. Photo-induced fragmentation of peptides and proteins has been studied in the gas phase, as both anions and cations, by mass spectrometry using UV lasers. The main findings of the previous studies are reviewed in the following. Then, outcome from the new field of VUV synchrotron radiation activation are discussed.

1. Previous laser based experiments

a. Aromatics

The wavelength delivered by the lasers is a key factor as it determines the site where photons are absorbed and therefore where the energy is deposited. Below 250 nm (4.96 eV), the main contribution to the UV absorption comes from the aromatic amino acids. Phenylalanine absorbs at 257 nm (4.82 eV), while tyrosine and tryptophane have onsets at 274 nm (4.52 eV) and 280 nm (4.43 eV), respectively. The nature of the lowest energy excited states of aromatic amino acids and of tryptophane in particular has been extensively studied at different levels of theory (Serrano-Andrés & Roos, 1996; Gindensperger *et al.*, 2010; Grégoire *et al.*, 2007). Most of the oscillator strength

is carried out by π - π^* transitions involving molecular orbital localized on the indole group. Those have been found in the 4.3 eV (288 nm) to 5.3 eV (234 nm) photon energy range depending on the level of theory and on the isomer considered. Electronic transitions between the HOMO located on the indole group and the σ^* on the amino group, appearing in the same energy range, possess a noticeable charge transfer character. Another charge transfer transition from the indole π orbital to a π^* located on the carbonyl was also found above 5.7 eV (217 nm). The relative energetic ordering of the lowest excited states for aromatic amino acids seemed to be very sensitive to the conformations (Grégoire *et al.*, 2007).

The aromatic amino acid spectral region has been probed for peptides by several groups using UV lasers in the 220 to 300 nm (5.64-4.13 eV) range (Antoine & Dugourd 2011; Gabryelski & Li 1999; Antoine *et al.*, 2006; Williams *et al.*, 1990; Oh *et al.*, 2005; Aravind *et al.*, 2012; Pérot *et al.*, 2010). Most of the authors have reported enhanced fragmentation in the vicinity of the chromophore along with side chain fragments from aromatic residue (Antoine *et al.*, 2006; Oh *et al.*, 2005; Gabryelski & Li 1999). The fragmentations observed for tryptophane have been rationalized on the basis of the nature of the excited states populated upon photoabsorption using a unique experimental arrangement, in which both the ion and its neutral losses are measured in coincidence (Grégoire *et al.* 2009; Lepere *et al.* 2007; Lucas *et al.* 2008). Transitions involving molecular orbitals localized on the indole group lead to C_α - C_β bond cleavage. This bond was cleaved too upon population of π^*_{CO} and σ^*_{NH} orbitals (Lucas *et al.* 2008). The π - π^*_{CO} transitions also lead to C_α -N bond breaking. Internal conversion has also been proposed to be partly responsible for the dissociation along the C_α -N and C_α - C_β bonds. These studies have shown that the photophysics of protonated tryptophane and aromatic amino acids in the near-UV is governed by the nature of the excited state populated by photoabsorption of the ions. Protonated peptides have been later probed with similar experimental approaches in which both the ionic and neutral fragments are detected (Pérot *et al.*, 2010; Aravind *et al.*, 2012). The mechanism, in which the active electron drives the fragmentations, has been extended to small peptides. Indeed, π - π^* transitions involving the aromatic side chain have been found mainly to produce C_α - C_β bonds breakage. The same fragmentations are observed when the active electron sits on the carbonyl close to the C terminal. In contrast, C_α -N fragmentations appear with the electron attached to the CO group near the N-terminal, which might account for the appearance of *c*- and *z*- sequence ions reported earlier (Gabryelski & Li, 1999; Oh *et al.*, 2005). Cleavage of the amide bond, producing *a*- and *y*- fragment ions, has found to occur following internal conversion, which seemed to be the most important relaxation pathway (Pérot *et al.* 2010).

Overall the fragmentations did not appear very abundant in comparison to CID and ECD (Antoine *et al.*, 2006), which might come from low cross section in this spectral region associated with localized chromophores.

b. Photodissociation at 193 nm & 157 nm

Excimer lasers deliver shorter wavelengths and thus have allowed other chromophores to be probed. Although at 193 nm (6.42 eV) aromatic sides chains have been shown to contribute to the electronic excitation of peptides, most of the cross section has been ascribed the peptidic bond (Bulheller *et al.*, 2008; Serrano-Andrés, 1996b, 1998, 2001).

This chromophore has been described as a four level system involving two doubly occupied π orbitals (π_1 and π_2), the oxygen lone-pair n_O and the antibonding π_3^* orbital. In this frame, the ordering of the lowest energy electronic transitions involving the peptidic backbone is $n_O \rightarrow \pi_3^*$ (W), $\pi_2 \rightarrow \pi_3^*$ (NV₁), and $\pi_1 \rightarrow \pi_3^*$ (NV₂). The $n_O - \pi_3^*$ transitions has been located around 5.5 eV (225 nm) with a weak oscillator strength. The intense absorption band around 6.5 eV (191 nm) has been assigned to $\pi_2 - \pi_3^*$ transition. The $\pi_1 - \pi_3^*$ transition has been located about 9.5 eV (130.5 nm). Charge transfer transitions involving molecular orbitals located on adjacent amino acids have been suggested to account for the 7.5 eV (165 nm) absorption band.

The first photoactivation at 193 nm on peptides goes back to the early 1980's (Bowers *et al.*, 1984; Lebrilla *et al.*, 1989; Hunt *et al.*, 1989). In the 90s, McLafferty has pioneered 193 nm photodissociation of electrosprayed protein ions (Williams & McLafferty 1990). The Biemann group also implemented 193 nm photodissociation as a MS/MS technique on a four sectors instrument (Martin *et al.*, 1990). Later on, Gorman and Amster (Gorman & Amster 1993) reported photodissociation at 193 nm in an FT-ICR instrument. Gimion-Kinsel and coworkers have used 193 nm photodissociation proteins in a two stage linear time-of-flight apparatus (Gimonkinsel *et al.*, 1995). It was not until 2004 that the Reilly group reported 157 nm (7.9 eV) photodissociation on a home-built tandem time-of-flight (ToF) mass spectrometer (Thompson *et al.*, 2004). Soon after Moon and coworkers (Moon *et al.*, 2005) reported photodissociation at 193 nm of some singly protonated peptides generated by matrix-assisted laser desorption/ionization (MALDI) using tandem time-of-flight mass spectrometry. For peptides with arginine at the C-terminus, x , v , and w fragment ions were generated preferentially while a - and d - fragment ions dominated for peptides with arginine at the N-terminus. These findings were confirmed subsequently (Choi *et al.*, 2006). The Reilly group (Cui *et al.*, 2005) reported from 157 nm photodissociation that when the charge was localized at the C-terminus of the peptide, x -, v -, and w -type fragments dominated the mass spectra. When the charge is sequestered at the N-terminus, a - and d -type ions were extremely abundant, as exemplified in figure 11 where the 157 and 193 nm photodissociation mass spectra of singly protonated substance P ions stored in a linear ion trap are compared (Thompson *et al.*, 2007). Both distributions at 193 and 157 nm looked overall similar. Evidence has been presented suggesting that the fragmentation occurred via photolytic radical cleavage of the peptide backbone at the bond between the alpha-carbon and carbonyl-carbons to form the a/x -sequence ions. A recent instrumental development combining a linear ion trap and an orthogonal-ToF has allowed time-dependent studies of the product ions generated by photodissociation (Kim *et al.*, 2009). Interestingly, this study concluded that following 157 nm photodissociation, x - and v - type fragments were the most abundant ions in the mass spectra up to 1 μ s after activation. The y - sequence ions being thermal in nature were reported to gain intensity soon after photoabsorption. The fragmentations observed at 157 nm laser excitation have been tentatively proposed to follow a Norrish type I reaction (Thompson *et al.*, 2004). In a combined theoretical and experimental study, Parthasarathi and coworkers (Parthasarathi *et al.*, 2010) have studied the effect of the removal of an electron on dipeptides and found that ionization of peptide cation substantially weakens the C_α -C backbone bond, which appeared in agreement with the observation of a/x - sequence ions upon 157 nm photodissociation. The authors postulated that the 157 nm photodissociation occurred following a Rydberg's state

excitation, which are known to converge to an ionic limit and thus possess some of the properties of the ions. However, this Rydberg state hypothesis contrasts with the rationalization of the electronic excited states of peptides found in the literature. The 193 nm (6.42 eV) absorption band has been suggested to involve mostly the π_2 - π_3^* (NV_1) transition (Serrano-Andrés, 1996, 1998, 2001), whereas the 157 nm (7.9 eV) excitation falls in charge transfer region and may involve π_2 located on one residue and the π_3^* located on an adjacent residue.

2. VUV photon-induced fragmentation

a. Previous SR studies

Using the setup described here above in part II.B.3.1, Schlathölter and coworkers have studied the photon-activation of protonated Leucine Enkephaline (LeuEnk) at several photon energies in the 8 to 40 eV range (Bari *et al.*, 2011). These authors have observed two fragmentation regimes for LeuEnk: below and above the photoionization threshold. At 8 and 9 eV the mass spectra were reported to be different from the rest of the photon energy range, being dominated by b_3/y_2 and immonium ions, with a weak a_4 ion. Tyrosine and phenyl-alanine side chain losses were also identified. Several internal fragments were assigned to rearrangement of the a_4 ion. The fragmentation patterns appeared to be partly similar to those reported earlier under collision activation conditions. The author suggested that these pathways originated from intramolecular vibrational redistribution of the energy. However, the strong neutral side chain losses involving the tyrosine and the tryptophane were analogous to the previously reported laser based experiment (Tabarin *et al.*, 2005), thus suggesting that excitations involving aromatic amino acids still bear an important oscillator strength in the VUV range. Above 9 eV, the spectra changed dramatically. The main fragments appeared to be immonium ions, internal fragments, and de-amination from further fragmentation from the a_4 sequence ion. At 20 eV series of a , b , and c fragments having lost the tyrosine side chain were produced. A three steps process, in which first the aromatic side chain is first non-ergodically fragmented and followed by backbone cleavage upon IVR, has been put forward. Density functional theoretical calculations for the protonated peptide have shown that the three highest occupied molecular orbital involved the aromatic rings. The authors suggested that upon photoionization, the ejection of an electron located on the aromatic side chains induced non-ergodic fragmentations of the C_α - C_β bond.

The same group has also investigated a series of polyglycine bearing a phenylalanine residue at the C-terminal and a tyrosine at the N-terminal, using the same setup in the 8 to 30 eV photon energy range (González-Magaña *et al.*, 2012). This allowed them to systematically probe the effect of peptide length on the fragmentation. Below 5 glycine units, the fragmentations involved aromatic side chain losses, indicative of the creation of positive hole on the glycine followed by charge migration toward the termini. For 10 glycines, side chain fragments were greatly reduced and doubly charge a - and b - ions were observed, thus suggesting that the hole-migration process was quenched.

b. SR activation of substance P

Using the coupling of a commercial linear ion trap (LTQ XL) with the DESIRS VUV beamline at the synchrotron SOLEIL (Milosavljević *et al.*, 2012c; Nahon *et al.*, 2012) described in part II.B.3.1, photoactivation of substance P (RPKPQQFFGLM-NH₂) has been investigated in the 5.6 eV (221 nm) to 20 eV (62 nm) range, a region that includes both previous 193 and 157 nm laser-based studies. The peptide was electrosprayed from water methanol (50:50) solution at 10 μM. Substance P has come out as a model peptide for activation methods (Fung *et al.*, 2009; Axelsson *et al.*, 1999; Debois *et al.*, 2006) and also laser-PD (Cui *et al.*, 2005; Thompson *et al.*, 2007, Barbacci & Russell 1999). Figure 12 shows MS/MS spectra of the [M + H]⁺ ions of substance P irradiated during 500 ms at three photon energies: 8, 11 and 15eV. In agreement with Bari *et al.*, (Bari *et al.*, 2011), two fragmentation regimes are distinguished: below and above the ionization threshold.

Below the ionization threshold. At 8 eV, the MS/MS spectrum in figure 12 shows neutral losses arising from the methionine (15 and 47 Da) and from the leucine (43 Da) (Zang & Reilly, 2009). Cleavage of the polypeptide backbone into *a*-type fragments ranging from *a*₄ to *a*₁₀ has also been observed with comparable ion abundances along the series. The corresponding *x*-type ions were absent as a consequence of the arginine position at *N*-terminal, which sequester the proton. These observations appear to be in agreement with the previous studies realized at 193 nm (6.4 eV) and 157 nm (7.9 eV) (Cui *et al.*, 2005; Thompson *et al.*, 2007) and which are reproduced in figure 11. Clearly, both experiments have produced similar distribution of *a*-type ions. The occurrence of the usual *a*₉+1 and *a*₁₀+1 fragment ions has been rationalized by Zang & Reilly (Zang & Reilly, 2009) and suggested to be due to the presence of a glycine residue, which limit the β-elimination reaction to form *a*- ions. A charge driven mechanism has been suggested to account for the observation of *y*- type ions on peptides containing an *N*- terminal arginine (Zang & Reilly, 2009). However a striking observation from figure 12 is the absence of the *d*-type ions that were abundant in the laser-based experiment (figure 11). Formation of these ions has certainly to be linked with the nature of light source, as possible non-linear excitation processes might appear with high-power lasers and which are ruled out with a soft, quasi continuous light source as SR. Additional experiments with variable laser power are necessary to provide a definitive answer.

Above the ionization threshold: dissociative Photoionization (DPI). At 11 eV, a major modification was observed on the mass spectrum (figure 12). The main product ion became the photoionized species [M + H]²⁺, which results from the loss of one electron. The ionization threshold has been reported at 10.26 eV for the singly protonated peptide (figure 8). Although the ionization energy for the glutamine amino acid, it is likely that the highest occupied molecular orbital lies on the methionine. Moreover, new fragments appeared, such as *y*₈, *x*₉, and side chain losses from the parent. Beside, the *a*- sequence ion series remains unaffected at this photon energy. This point questions seriously the Rydberg excitation hypothesis (Parthasarathi *et al.*, 2010) discussed in part III.B.1.2, as it is unlikely to find series above their ionization limit. In contrast, valence electronic excitations still bear noticeable oscillator strength near the ionization threshold (Berkowitz J., 1979).

At 15 eV, the quantity and the abundance of the fragments increased dramatically, while the main product remained the [M + H]²⁺. These mass spectra

revealed important changes in the fragmentation processes concomitant with the appearance of the photoionized species $[M + H]^{2+}$ and $[M + H]^{3+}$, as previously reported by Zubarev and Yang under electron impact ionization (Zubarev & Yang, 2010). The origin of this multiply ionized species is not clear but arises likely from sequential ionization of the products. The second most abundant ion for 15 eV irradiation corresponded to the photoionized species but with a loss of 74 Da corresponding to the loss of $\text{CH}_2=\text{CHSCH}_3$, which is the side chain of the methionine. This neutral loss had been previously observed from electron-induced dissociation (EID) of substance P (Fung *et al.*, 2009) but not from photodissociation (Zang & Reilly, 2009). Hence, it is certainly related to photoionization on the methionine side chain. Numerous other sequence ions are also presents at 15 eV, resulting from the backbone cleavage. The *a*-type series is still present along with new *b*-, *c*-, *x*-, *y*- and *z*-type fragments. Series of doubly charged fragment ions appear clearly together with neutral losses from the radical cation. First all appearance of doubly charged fragments and of new C-terminal ions obviously related to the photoionization process, which create an additional charge on the peptide. Hence, dissociative photoionization and related electron impact dissociation (EID) enriched the nature of sequence ions by this process and should produce enhanced sequence coverage. It has been shown theoretically (Parthasarathi *et al.*, 2010) that the formation of a radical cation on the peptidic backbone weakens substantially the $\text{C}_\alpha\text{-C}$ bond and to a lesser extends, both C-N and N-C_α bonds. Hence, the appearance of *b*-/*y*- and *c*-/*z*- sequence ions upon ionization originates partly from ionization of the peptidic backbone. The absence of side chain losses accompanying the sequence ion is striking for Substance P (11 amino acids) as compared to Leucine Enkephaline (Bari *et al.*, 2011) but it is in line with the polyglycine studies (Gonzalez-Magaña *et al.*, 2012). Figure 13 reproduces the EID tandem mass spectra of Substance P reported by the Zubarev group (Fung *et al.*, 2009). The photon induced fragments produced at 15 eV above the ionization threshold of the $[M + H]^+$ (figure 12) are very similar to those generated by EID (Figure 13) (Fung *et al.*, 2009). This observation confirms that similar mechanisms of fragmentation are involved in EID and in VUV dissociation photoionization (DPI) and are very likely driven by the same radical mechanisms. Moreover our results are consistent with those obtained by Laskin and collaborators on $[M + H]^{2+}$ peptide ions studied by SORI-CID (Laskin *et al.*, 2007). Their MS/MS spectra showed different losses of small molecules from the side chains of the amino acids and formation of *a*-type fragments. Recently Kalcic and coworkers (Kalcic *et al.*, 2009, 2012) have submitted a synthetic phosphopeptide to femtosecond laser induced dissociation (fs-LID). Full sequence coverage with abundant *a*-, *b*-, *c*-, *x*-, *y*-, and *z*-type sequence ions was reported. The fs-LID process is initiated by tunneling ionization leading to formation of the $[M+H]^{2+}$ radical cation. It may be concluded, that dissociative photoionization (DPI) using SR is very similar in nature to EID (Fung *et al.*, 2009) and fs-LID (Kalcic *et al.*, 2009, 2012). The radical cation produced is subject to proton and radical directed fragmentation, thus leading to abundant and various sequence ions. The large amount of fragments of different nature allows obtaining redundant information on peptide sequence.

3. Soft X-rays photon-induced fragmentation

The group of Thomas Schlatholter has recently investigated the fragmentation induced upon carbon K-shell excitation on leucine enkephaline (Gonzalez-Magaña *et al.*, 2012). The photon energy region investigated spanned from the onset at 284 eV up to 300 eV. The mass spectra appeared dominated by immonium ions (Y and F) and some fragments of the aromatic side chains. These ions had also been found in VUV activation spectra above 15 eV (Bari *et al.*, 2011). The backbone fragments (a_2 , b_2 , b_3 and c_2), stripped off the tyrosine side chain formed under VUV irradiation, were also observed at the C K-edge. The photofragmentation spectra show features in agreement with EXAFS literature data and with previous work described in part III.1.3 (Milosavljević *et al.*, 2012a). The $C1s \rightarrow \pi^*_{\text{aromatic}}$ excitation was found to be the softest channel, leading predominantly to large fragments. In contrast the $C1s \rightarrow \pi^*_{C=O}$ transition contributed more the formation of smaller fragments. Overall, the fragmentation patterns were not found to be very different from those produced upon valence excitations.

IV. PHOTOACTIVATION OF MULTIPLY DEPROTONATED BIOLOGICAL IONS: ELECTRON PHOTODETACHMENT SPECTROSCOPY

A. Previous laser based experiments

Dugourd, Antoine and coworkers (Antoine & Dugourd, 2011) have recently reviewed their abundant and pioneering work on photon activation of anions in the near ultraviolet range. Using tunable UV lasers, they have extensively studied the spectroscopy of stored multiply negative ions of peptides (Antoine *et al.*, 2006; Joly *et al.*, 2008, 2007), proteins (Bellina *et al.*, 2010, Joly *et al.*, 2007), nucleic acids (Gabelica *et al.*, 2007a, 2007b, 2006), and carbohydrates (Enjalbert *et al.*, 2012). As mentioned above (part III.B.1), the wavelength range (down to 210 nm) involved in these studies was restricted to the electronic excitation localized on aromatic amino acids with little contribution from the disulfide bond (Kelly *et al.*, 2005). It appeared that, following photoabsorption, the main relaxation channel involved electron detachment. For proteins and peptides, the onset of electron photodetachment occurred at low photon energy and apparently coincided with the photoabsorption bands measured by UV spectroscopy on samples in solution. A photophysical model has been proposed in which photodetachment was mediated by a discrete electronic excited state that crosses with an autoionising state, if the photon energy was larger than the sum of the electron binding energy plus the repulsive Coulomb barrier. This model was tested and validated in the near UV for peptides and nucleic acids. As a consequence, electron photodetachment spectroscopy was found to mirror the lowest electronic excited state of the anions in the gas phase, thereby providing a mean of accessing optical near-UV absorption spectroscopy of large biomolecular anions in the gas phase.

B. Ion trap synchrotron radiation studies

Electron photodetachment spectroscopy has been probed further in the VUV for carulein, a sulfated peptide, melittin and insulin using the coupling of the LTQ XL and a VUV beamline described in part II.B.3.2. Electron detachment remained the main relaxation channel in the 4.5 to 20 eV range (Brunet *et al.* 2012). Observation of

resonances on the photodetachment yields, which correspond closely to electronic transitions reported for peptides (Serrano-Andrés, 1996, 1998, 2001), indicated that the two steps photophysical model for photodetachment was still valid in an extend wavelength range. Investigations on the doubly deprotonated carulein (a sulfated peptide) revealed that the main fragmentations were a_7 , a_8 , and a_9 -sequence ions accompanied by abundant tryptophane, CO₂ and SO₃ losses from the oxidized species (Brunet *et al.*, 2012). The fragmentation pattern did not evolve much in the 5.5 to 20 eV range. This is in contrast with the case of protonated peptides, for which new channels open above the ionization threshold. The oxidized ions produced at various photon energies have been further probed by CID in a MS³ experiment. The fragmentation profiles remained unaffected by the initial photon energy, indicating that, on the time scale of the experiment, the memory of the initial electronic excited state was lost. Moreover, the fragmentation efficiency increased with the photon energy. For carulein, the main fragmentation involved neutral losses and a -ion formation.

Implementation of a quadrupled Nd:YAG laser in a two-color non resonant arrangement was used to prepare oxidized species of proteins and peptide inside the ion trap. These species were then submitted to SR activation to probe their spectroscopy (Brunet *et al.*, 2011, 2012). It appeared that anionic peptides bearing tryptophan and tyrosyl radical showed very similar photodetachment yields as their closed-shell counterparts. Interestingly, these oxidized species exhibited unexpected higher photofragmentation yields increased by one order of magnitude as compared to the closed-shell anion of same charge. It is noteworthy that this two-color (laser + SR, i.e. UV + VUV) combination represents a unique arrangement to access the spectroscopic properties of radicals.

V. CONCLUSIONS

The field of trapped ion spectroscopy using synchrotron radiation is in its infancy, but rapidly growing and should very soon impact a very broad trans-disciplinary community at the interface of physics, chemistry and biology, including radiobiology and astrobiology. The coupling of ion traps with VUV and soft X-ray beamlines at synchrotron radiation facilities complement existing techniques for ion spectroscopy and also brings the possibility to perform electronic spectroscopy of biological species placed in the gas phase by electrospray, an extremely powerful method of preparing the precursor ion. Especially, the two-colors scheme used to prepare and probe the spectroscopy of radical anion appears as a very promising tool. The study of ionization energies of peptides and proteins has revealed unexpected correlation between this fundamental physical property and the gas phase structure of the target. Synchrotron radiation complement nicely, in the short wavelength domain, previously existing laser-based works on both cations and anions. The fragmentations of protonated peptides may now be studied over an extended wavelength range with access for the first time to a manifold of electronic excited state that was not possible otherwise. The tunability of SR allows continuously bridging the gap between unrelated activations methods, such as laser PD and EID, since it allows ion activation in a controlled manner with a precisely known-energy deposition into the system. A deeper understanding of the

photophysics has come from laser-based experiments on small system in the near UV, where photoabsorption is localized around aromatic amino acids. Although the situation gets more complicated at higher photon energy, a clearer understanding of short-wavelength photodynamic should emerge in a near future from synchrotron radiation-based studies up to the soft X-ray regime.

ACKNOWLEDGEMENTS

This work was supported by the Agence Nationale de la Recherche Scientifique, France, under the project # ANR-08-BLAN-0065 and partially by “Pavle Savic” project of bilateral scientific collaboration between Serbia and France. A.M. acknowledges the support by the Ministry of Education and Science of Republic of Serbia (Project No. 171020) and the COST Action MP1002 (Nano-IBCT). The SOLEIL synchrotron radiation facility is acknowledged.

BIOGRAPHY

Alexandre Giuliani obtained a PhD in 2003 from the *Université de Liege* (Belgium) under the supervision of Dr. Marie-Jeanne Hubin-Franskin and Prof. Jacques Delwiche in molecular spectroscopy using electron energy loss and photoabsorption methods. After a two years post-doctoral stay at the *Institut de Chimie des Substances Naturelles* in the laboratory of Prof. Olivier Laprévotte, where he learnt analytical mass spectrometry, he joined INRA (*Institut National de la Recherche Agronomique*) in 2006 to work at the SOLEIL synchrotron radiation facility, where he is on secondment at present. His main interests are atmospheric pressure photoionization and spectroscopy of trapped ions.

Aleksandar R. Milosavljević received his Ph.D. in atomic and molecular physics from University of Belgrade, Serbia in 2006, where he worked on electron interaction with biologically relevant molecules and electron transmission through insulating nanocapillaries. He then moved to SOLEIL synchrotron, France where he worked on developing novel experimental setup for synchrotron radiation tandem mass spectrometry. Currently he is working as an associate research professor at the Institute of Physics, University of Belgrade, Serbia in the field of atomic, molecular and chemical physics and collaborating in projects at SOLEIL on VUV and X-ray spectroscopy of trapped biopolymer ions.

Dr. Francis Canon is researcher at the INRA (*Institut National de la Recherche Agronomique*) and works at the CSGA (*Centre des Sciences du Goût et de l'Alimentation*) in Dijon, France. He received his PhD in biochemistry from the CIESSA (*Centre international d'études supérieures en sciences agronomiques*) at Montpellier in 2010. Afterwards, he was a postdoctoral researcher at the synchrotron SOLEIL using mass spectrometry coupled to synchrotron radiation to study proteins. Now, his scientific focus is on salivary protein interactions.

After a PhD in atomic and molecular physics obtained in 1991 at Orsay University (France), and a post-doc at UC Berkeley (USA), **Laurent Nahon** joined the CEA to work at the French synchrotron radiation facility LURE in charge first of the scientific

program of a UV-Free Electron Laser, and then as project manager of the VUV beamline SU5. Since 2005 he is seconded to SOLEIL, as the beamline group leader of the VUV high resolution, variable polarization DESIRS beamline. His main current scientific interests include : (i) interaction between circularly polarized VUV photons and chiral systems, leading to asymmetric photophysical or photochemical photon-induced processes, (ii) spectroscopy and fragmentation of state-selected cations (produced by photoionization of a neutral) and m/z -selected ionic biopolymers, (iii) Ultra-high resolution absorption spectroscopy on astrophysically-relevant small molecular systems.

Figure 1. Synchrotron radiation (SR) chemistry as a bridge between radiation chemistry and photochemistry. The dipole oscillator strength df/dE is shown as a function of wavelength and photon energy. A typical generic SR emission spectrum is presented covering the range from THz up to hard X-rays. The emission energy of common laboratory line source are indicated by arrows. Reprinted from (Hatano, 1999).

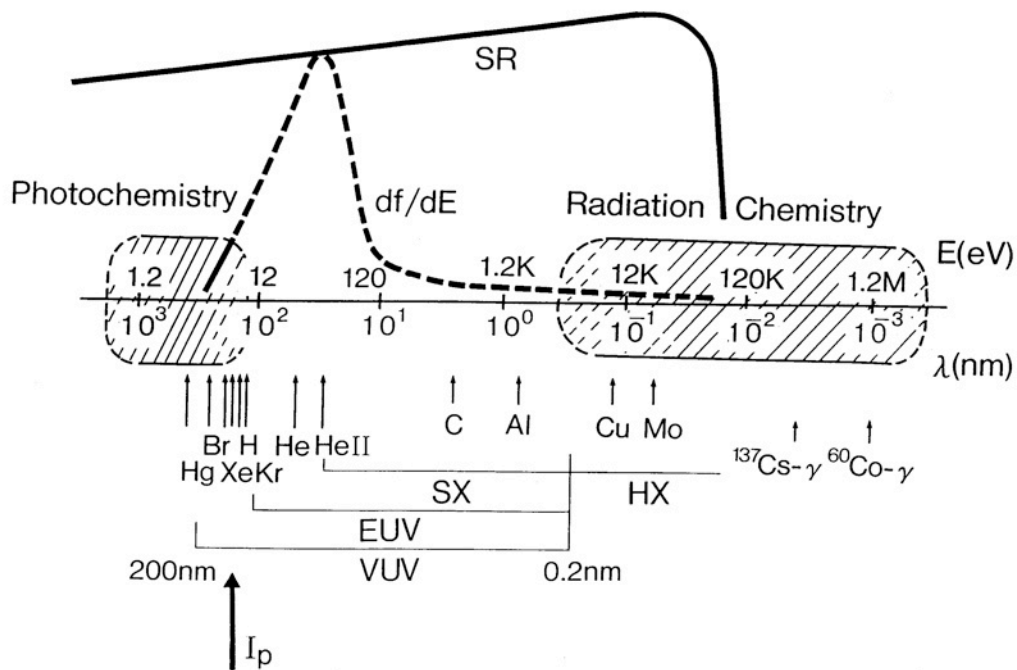


Figure 2. Principle of the merged-beam setup at ASTRID. Storage ring: I, ECD: ion source, EL: Einzel lens, M1 and M2: deflection magnets, ED: electrostatic deflector, IC: interaction chamber, FC1,FC2 and FC3: Farraday cups, PD: photodiode, D1 and D2 are particule sensors. Reprinted from (Kjeldsen, 2006).

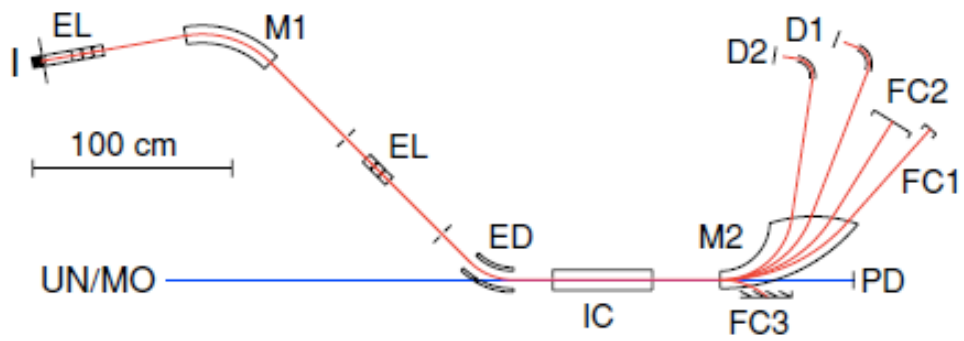


Figure 3. Schematic drawing of the ICR cell of MICRA. Reproduced from (Mauclaire *et al.*, 2004).

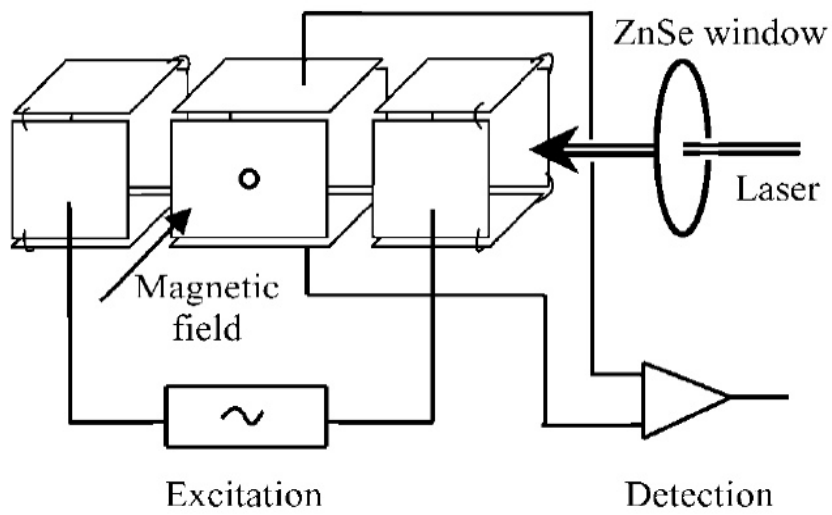


Figure 4. Temporal sequence of event in the Xe^+ ion photoionization experiment using MICRA. Reproduced from (Thissen *et al.*, 2008).

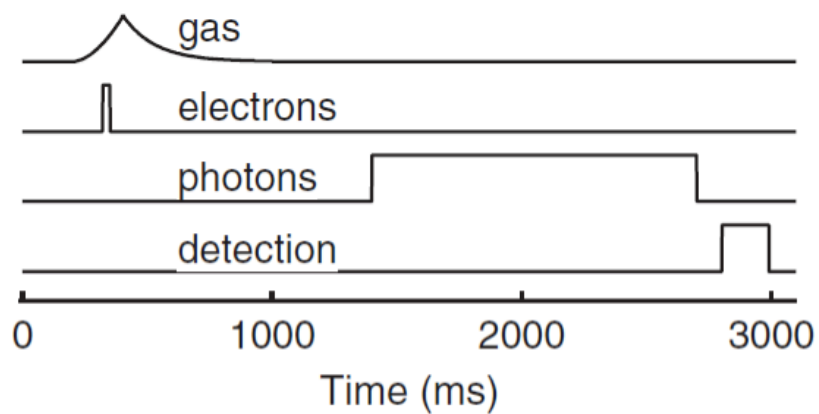


Figure 5. Schematic view of the coupling of a linear ion trap with a synchrotron radiation beamline at BESSY II. Reproduced from (Hirsch *et al.*, 2009).

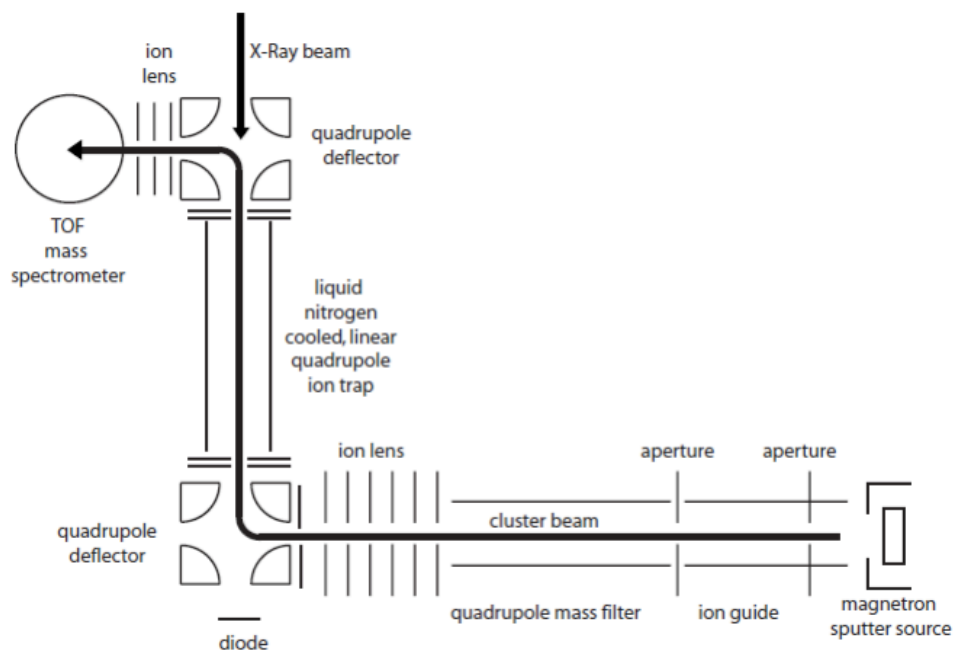


Figure 6. Experimental setup coupled to a VUV beamline at Bessy II. Reproduced from (Bari *et al.*, 2011).

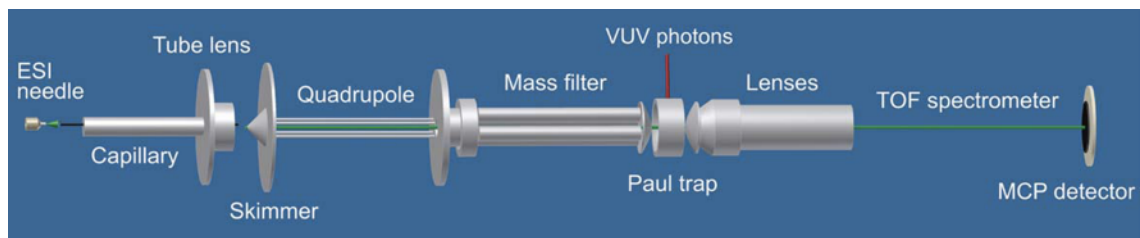


Figure 7. Schematic of coupling a LTQ XL with the DESIRS beamline at the SOLEIL synchrotron radiation facility. Reproduced from (Milosavljević *et al.*, 2012c).

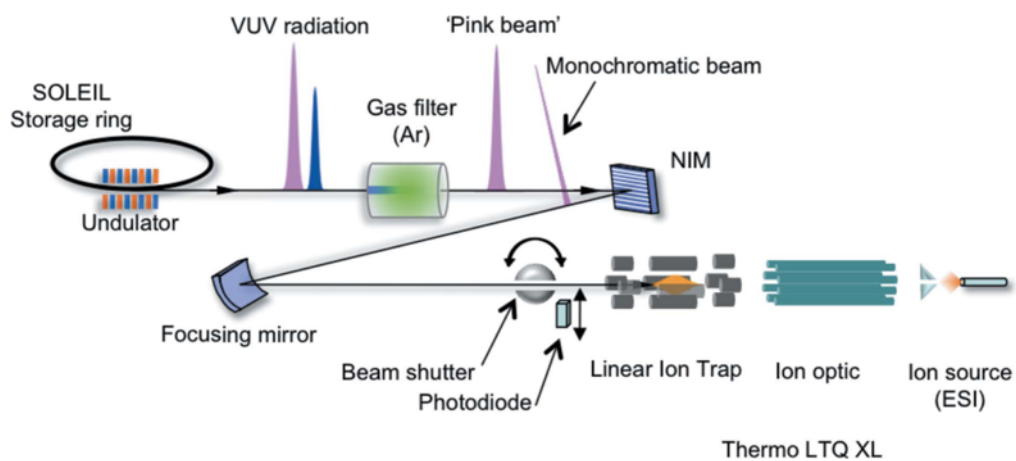


Figure 8. Ionization energies as a function of charge states. Data measured by electron impact are labeled as EI and come from (Budnik *et al.*, 2002). Full symbol measured by VUV photoionization are take from (Giuliani *et al.*, 2012).

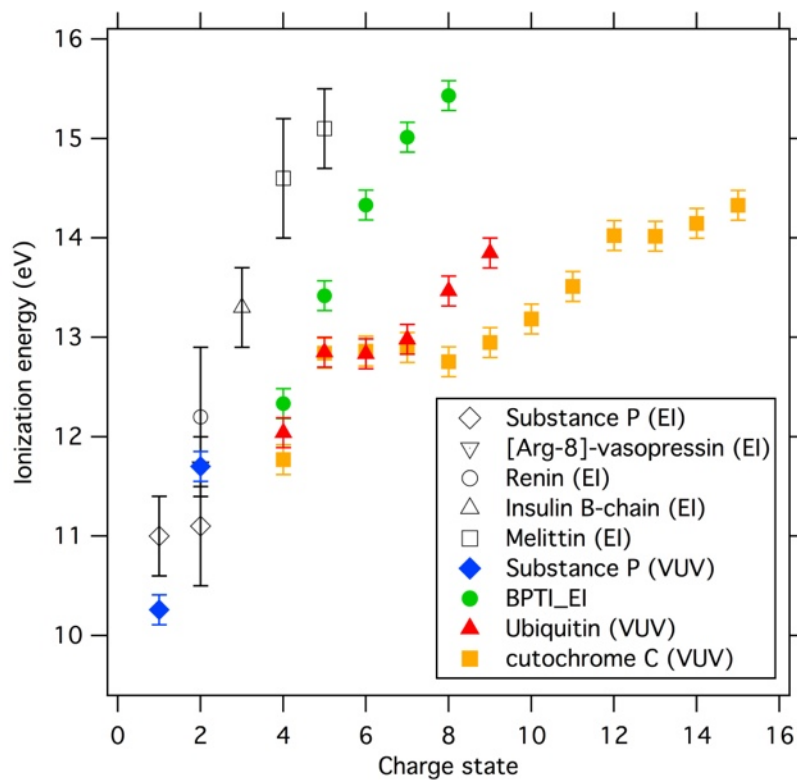


Figure 9. Comparison of experimental collision cross section from ion mobility (Shelimov *et al.*, 1997) as a function of the charge states for cytochrome C with the mean radius extracted from the ionization energy model. Figure adapted from (Giuliani *et al.*, 2012).

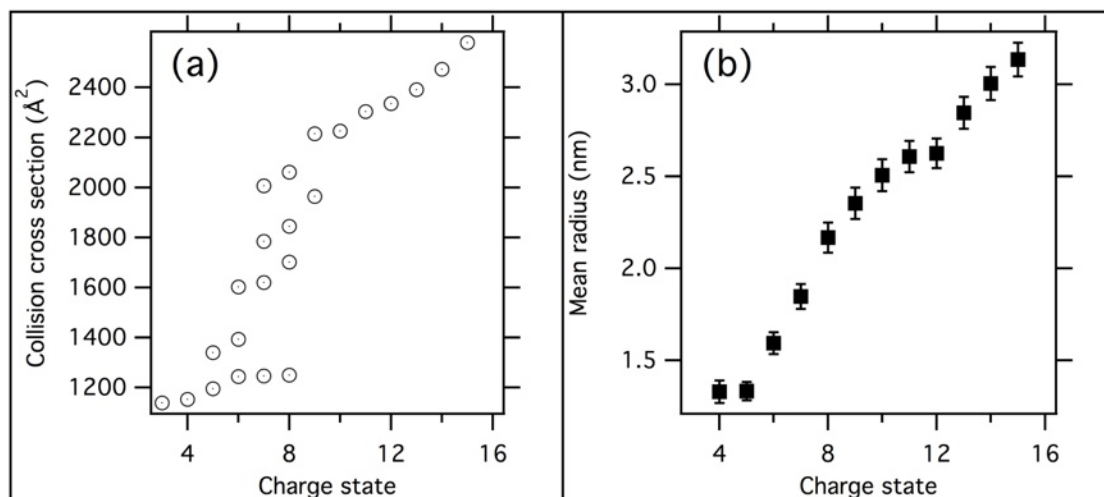


Figure 10. a–c) C, N, and O K-edge photoionization yields of the singly and doubly ionization of the 8+ precursor of equine cytochrome C. Vertical lines indicates K-shell ionization thresholds for glycyl-glycine. (d) Top panel: C K-edge total photoionization ion yield (TIY, m/z 1000–1400). (d) Bottom panel: Comparison of M^{9+} and M^{10+} C K-edge photoionization yields with corresponding $[M-CO_2]^{9+}$ and $[M-CO_2]^{10+}$ yields normalized to the same intensity at higher photon energies. Reproduced from (Milosavljević *et al.*, 2012a).

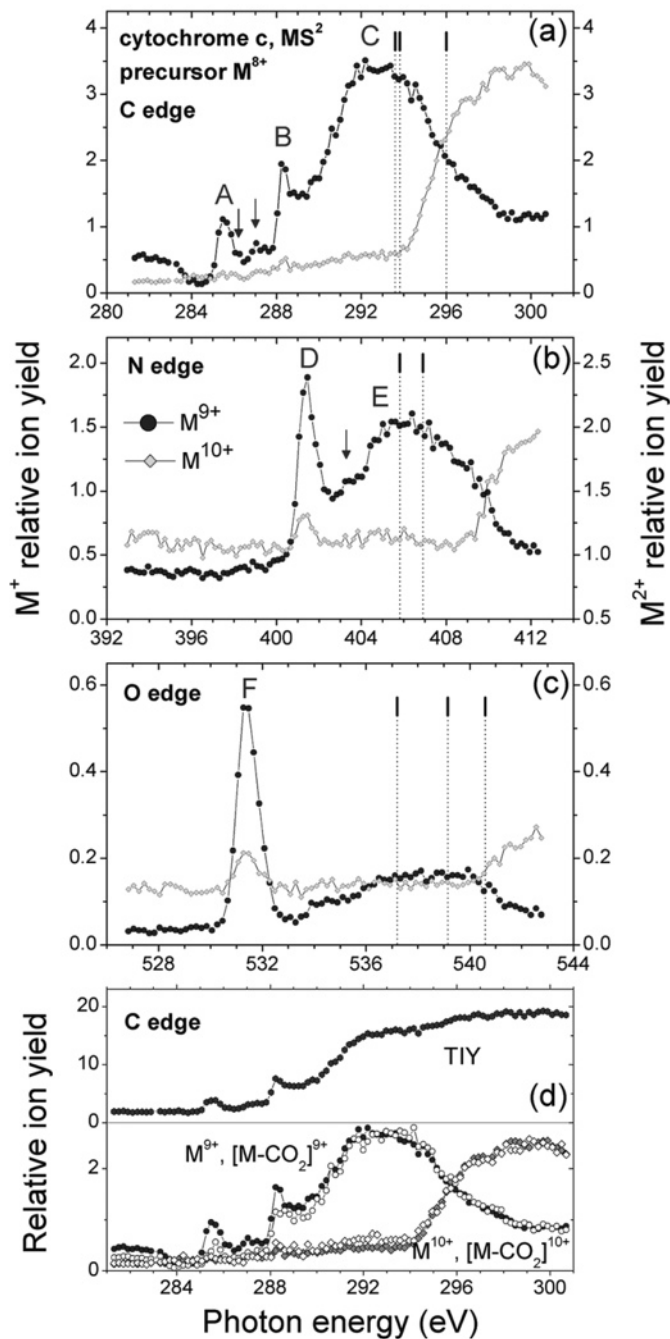


Figure 11. Linear ion trap photodissociation tandem mass spectra of Substance P (RPKPQQFFGLM-NH₂) using (a) 193 and (b) 157 nm excitation, reproduced from (Thompson *et al.*, 2007).

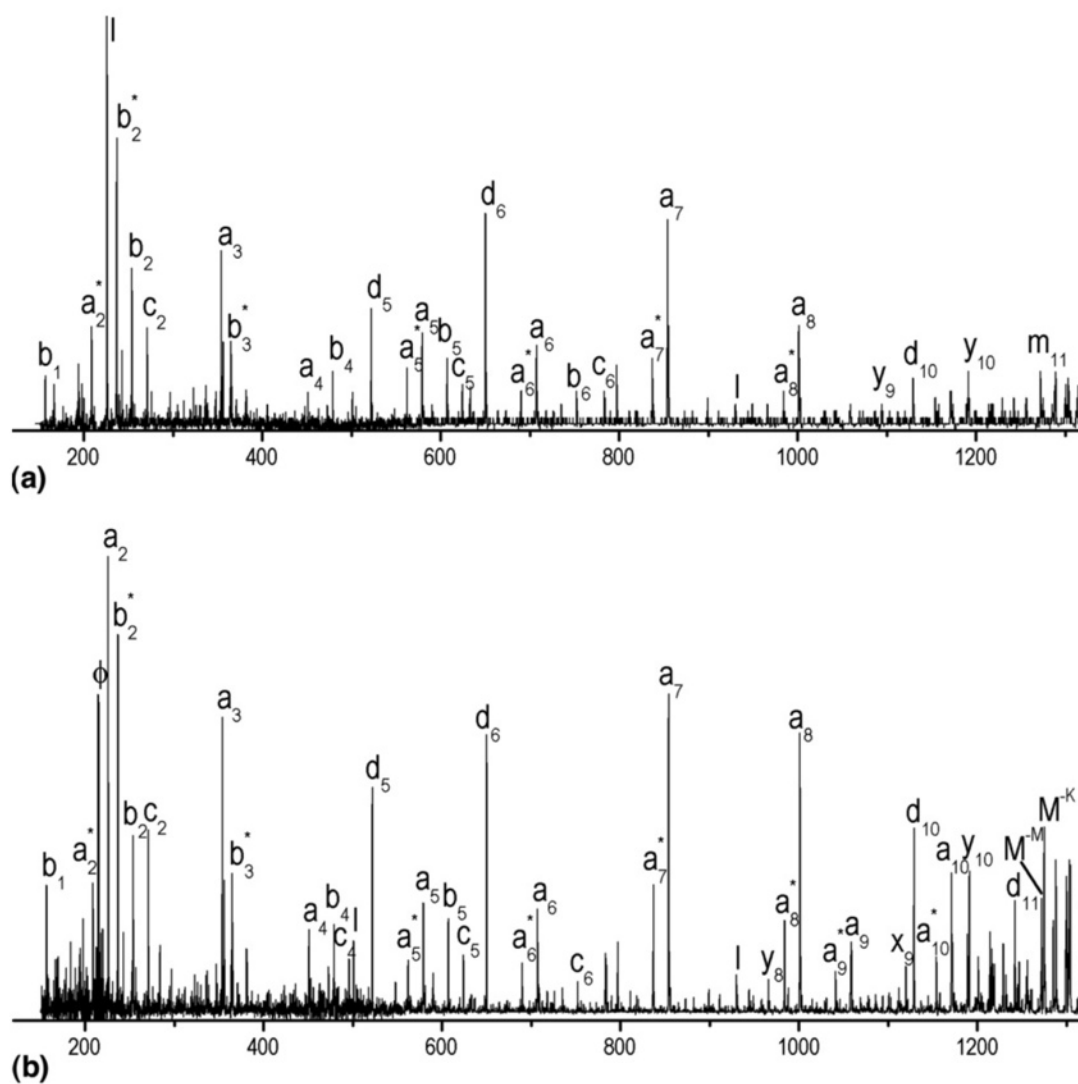


Figure 12. Linear ion trap VUV activation tandem mass spectra of substance P (RPKPQQFFGLM-NH₂) at three photon energies.

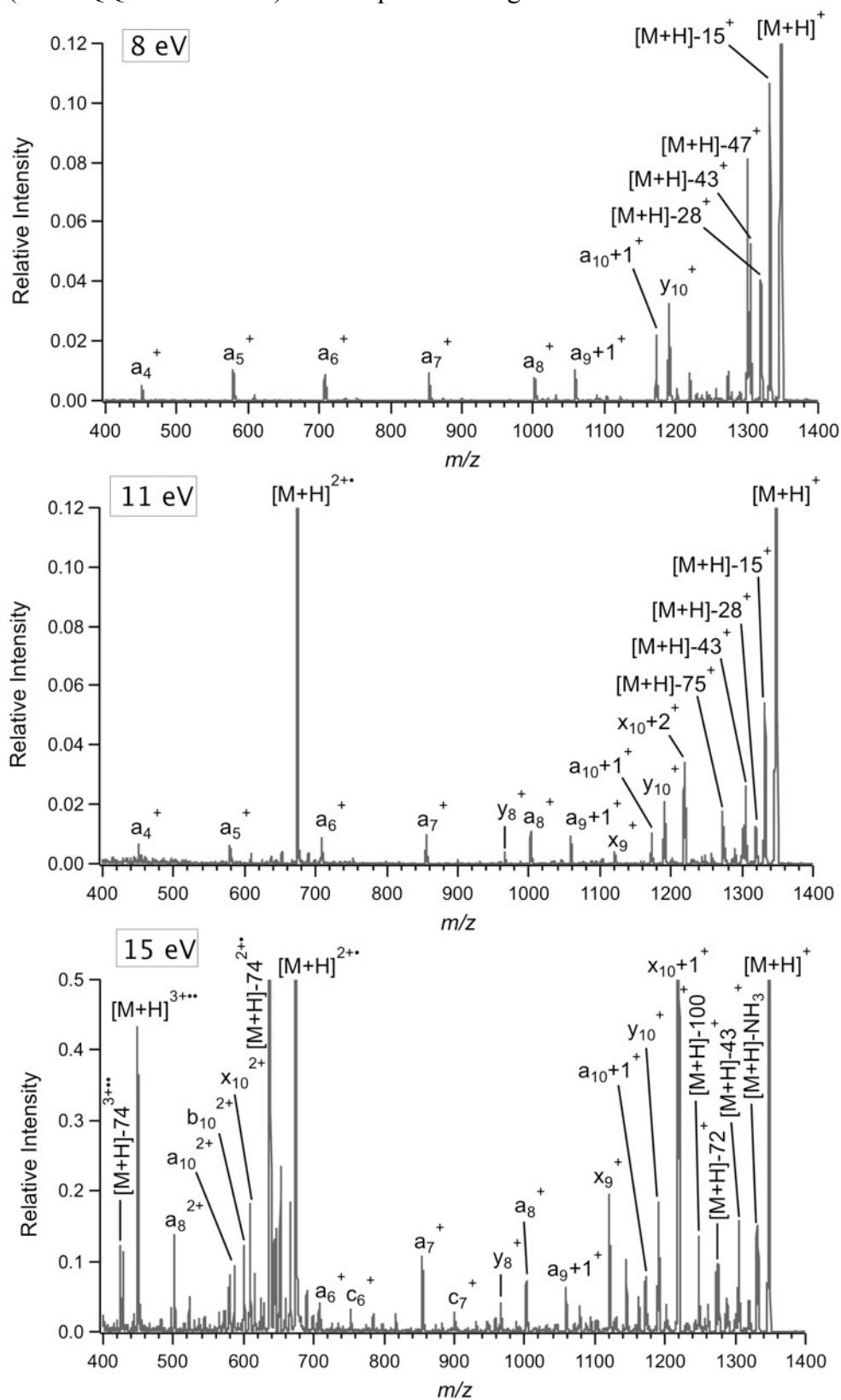
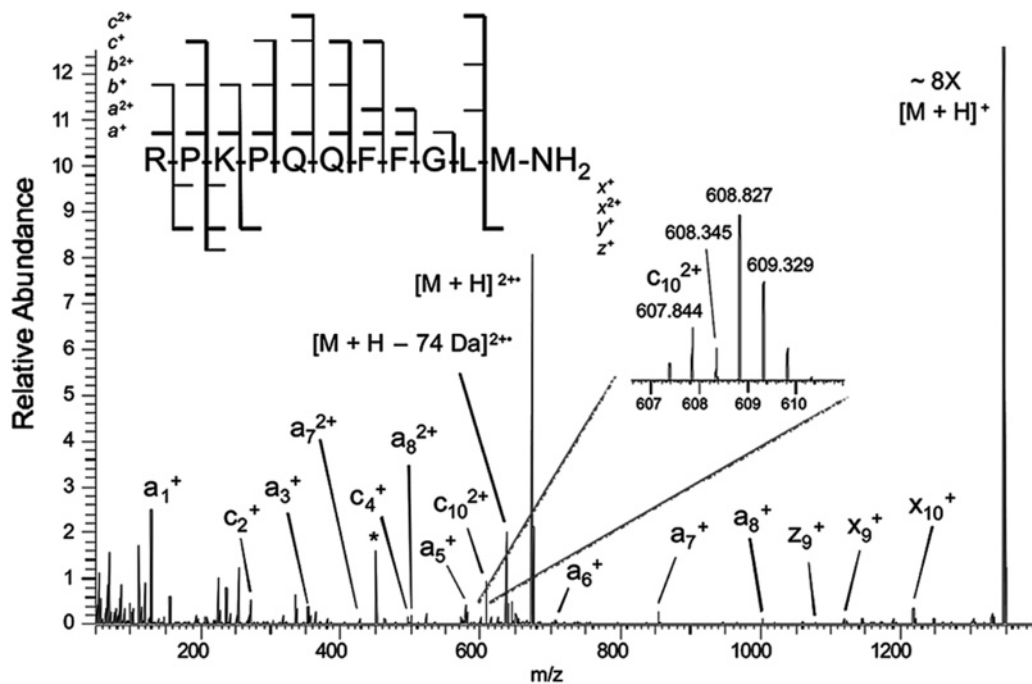


Figure 13. EID tandem mass spectrum of singly protonated substance P. (Inset) Isotopic distribution of c_{10}^{2+} ions. Reprinted from (Fung *et al.*, 2009).



REFERENCES

- Akiyama S, Takahashi S, Kimura T, Ishimori K, Morishima I, Nishikawa Y, Fujisawa T. 2002. Conformational landscape of cytochrome c folding studied by microsecond-resolved small-angle x-ray scattering. *Proc. Natl. Acad. Sci. U.S.A* **99**: 1329.
- Andersen T, Kjeldsen H, Knudsen H, Folkmann F. 2001. Absolute cross section for photoionization of CO⁺ leading to long lived metastable CO₂⁺. *J. Phys. B: At., Mol. Opt. Phys.* **34**: L327–32.
- Antoine R, Dugourd P. 2011. Visible and ultraviolet spectroscopy of gas phase protein ions. *Phys. Chem. Chem. Phys.* **13**: 16494.
- Antoine R, Broyer M, Chamot-Rooke J, Dedonder C, Desfrancois C, Dugourd P, Grégoire G, Jouvét C, Onidas D, Poulain P, Tabarin T, van der Rest G. 2006. Comparison of the fragmentation pattern induced by collisions, laser excitation and electron capture. Influence of the initial excitation. *Rapid Commun. Mass Spectrom.* **20**: 1648–52.
- Aravind G, Klærke B, Rajput J, Toker Y, Andersen L H, Bochenkova A V, Antoine R, Lemoine J, Racaud A, Dugourd P. 2012 Photodissociation pathways and lifetimes of protonated peptides and their dimers . *J. Chem. Phys.* **136** : 014307
- Axelsson J, Palmblad M, Håkansson K, Håkansson P. 1999. Electron capture dissociation of substance P using a commercially available Fourier transform ion cyclotron resonance mass spectrometer *Rapid Commun. Mass Spectrom.* **13**: 474–7.
- Badman E, Myung S, Clemmer D. 2005. Evidence for unfolding and refolding of gas-phase cytochrome c ions in a Paul trap. *J. Am. Soc. Mass Spectrom.* **16**: 1493–7.
- Barbacci D, Russell D. 1999. Sequence and side-chain specific photofragment (193 nm) ions from protonated substance P by matrix-assisted laser desorption ionization time-of-flight mass spectrometry *J. Am. Soc. Mass Spectrom.* **10**: 1038–40.
- Bari S, Gonzalez-Magaña O, Reitsma G, Werner J, Schippers S, Hoekstra R and Schlathölter T. 2011. Photodissociation of protonated leucine-enkephalin in the VUV range of 8–40 eV. *J. Chem. Phys.* **134**: 024314.
- Bellina B, Compagnon I, Joly L, Albrieux F, Allouche A R, Bertorelle F, Lemoine J, Antoine R, Dugourd P. 2010. UV spectroscopy of entire proteins in the gas phase. *Int. J. Mass Spectrom.* **297**: 36–40.
- Berkowitz J. 1979. Photoabsorption, photoionization, and photoelectron spectroscopy. New York: Academic Press. P.5-13.
- Bizau JM, Blancard C, Coreno M, Cubaynes D, Dehon C, Hassan El N, Folkmann F, Gharaibeh MF, Giuliani A, Lemaire J, Milosavljević AR, Nicolas C, Thissen R. 2011. Photoionization study of Kr⁺ and Xe⁺ ions with the combined use of a merged-beam set-up and an ion trap. *J. Phys. B: At., Mol. Opt. Phys.* **44**: 055205.
- Bizau J, Cubaynes D, Richter M, Wuilleumier F, Obert J, Putaux J, Morgan T, Källne E, Sorensen S, Damany A. 1991. First observation of photoelectron spectra emitted in the photoionization of a singly charged-ion beam with synchrotron radiation. *Phys. Rev. Lett.* **67**: 576–9.
- Bowers WD, Delbert SS, Hunter RL And Mciver RT. 1984. Fragmentation of Oligopeptide Ions Using Ultraviolet-Laser Radiation and Fourier-Transform Mass-Spectrometry. *J. Am. Chem. Soc.* **106**: 7288–9.

- Brodbeck J S. 2011. Shedding Light on the Frontier of Photodissociation. *J. Am. Soc. Mass Spectrom.* **22**: 197–206
- Brunet C, Antoine R, Allouche A-R, Dugourd P, Canon F, Giuliani A, Nahon L. 2011. Gas phase Photo-Formation and Vacuum UV Photofragmentation Spectroscopy of Tryptophan and Tyrosine Radical-Containing Peptides. *J Phys Chem A.* **115**: 8933–9.
- Brunet C, Antoine R, Dugourd P, Canon F, Giuliani A, Nahon L. 2012. Formation and Fragmentation of Radical Peptide Anions: Insights from Vacuum Ultra Violet Spectroscopy. *J. Am. Soc. Mass Spectrom.* **23**: 274–81.
- Budnik BA, Zubarev RA. 2000. MH₂⁺ ion production from protonated polypeptides by electron impact: observation and determination of ionization energies and a cross-section. *Chem. Phys. Lett.* **316**: 19–23.
- Budnik BA, Tsybin YO, Håkansson P, Zubarev RA. 2002. Ionization energies of multiply protonated polypeptides obtained by tandem ionization in Fourier transform mass spectrometers. *J Mass Spectrom.* **37**: 1141–4.
- Bulheller BM, Miles AJ, Wallace BA, Hirst JD. 2008. Charge-Transfer Transitions in the Vacuum-Ultraviolet of Protein Circular Dichroism Spectra. *J. Phys. Chem. B.* **112**: 1866–74.
- Choi KM, Yoon H, Sun M, Oh JY, Moon JH, Kim MS. 2006. Characteristics of photodissociation at 193 nm of singly protonated peptides generated by matrix-assisted laser desorption ionization (MALDI). *J. Am. Soc. Mass Spectrom.* **17**: 1643–53.
- Clemmer D, Hudgins R, Jarrold M. 1995. Naked Protein Conformations - Cytochrome-C in the Gas-Phase. *J. Am. Chem. Soc.* **117**: 10141–2.
- Close DM. 2011. Calculated Vertical Ionization Energies of the Common α -Amino Acids in the Gas Phase and in Solution. *J Phys Chem A.* **115**: 2900–12.
- Cotter RJ. 1984. Lasers and mass spectrometry. *Anal Chem.* **56**: 485A–504A.
- Covington A, Aguilar A, Covington I, Gharaibeh M, Hinojosa G, Shirley C, Phaneuf R, Álvarez I, Cisneros C, Dominguez-Lopez I, Sant'Anna M, Schlachter A, McLaughlin B, Dalgarno A. 2002. Photoionization of Ne⁺ using synchrotron radiation. *Phys. Rev. A.* **66**: 062710.
- Cui W, Thompson M, Reilly J. 2005. Pathways of peptide ion fragmentation induced by vacuum ultraviolet light. *J. Am. Soc. Mass Spectrom.* **16**: 1384–98.
- Debois D, Giuliani A, Lapr votte O. 2006. Fragmentation induced in atmospheric pressure photoionization of peptides. *J Mass Spectrom.* **41**: 1554–60.
- Dehmelt H, Jefferts K. 1962. Alignment of the H₂⁺ Molecular Ion by Selective Photodissociation. I. *Phys Rev.* **125**: 1318–22.
- Douglas D J, Frank A J, Mao D. 2004. Linear ion traps in mass spectrometry. *Mass Spectrom Rev.* **24**: 1–29.
- Dunbar R. 1971. Photodissociation of CH₃Cl⁺ and N₂O⁺ Cations. *J. Am. Chem. Soc.* **93**: 4354–59.
- Enjalbert Q, Racaud A, Lemoine J, Redon S, Ayhan M M, Andraud C, Chambert S, Bretonniere Y, Loison C, Antoine R, Dugourd P. 2012. Optical Properties of a Visible Push–Pull Chromophore Covalently Bound to Carbohydrates: Solution and Gas-Phase Spectroscopy Combined to Theoretical Investigations. *J. Phys. Chem. B.* **116**: 841–51.
- Fung YME, Adams CM, Zubarev RA. 2009. Electron Ionization Dissociation of Singly and Multiply Charged Peptides. *J. Am. Chem. Soc.* **131**: 9977–85.
- Gabelica V, Rosu F, Pauw E, Antoine R, Tabarin T, Broyer M, Dugourd P. 2007a. Electron photodetachment dissociation of DNA anions with covalently or noncovalently bound chromophores. *J. Am. Soc. Mass Spectrom.* **18**: 1990–2000.

Gabelica V, Rosu F, Tabarin T, Kinet C, Antoine R, Broyer M, De Pauw E, Dugourd P. 2007b. Base-Dependent Electron Photodetachment from Negatively Charged DNA Strands upon 260-nm Laser Irradiation. *J. Am. Chem. Soc.* **129**: 4706–13.

Gabelica V, Tabarin T, Antoine R, Rosu F, Compagnon I, Broyer M, De Pauw E, Dugourd P. 2006. Electron Photodetachment Dissociation of DNA Polyanions in a Quadrupole Ion Trap Mass Spectrometer. *Anal Chem.* **78**: 6564–72.

Gabryelski W, Li L. 1999. Photo-induced dissociation of electrospray generated ions in an ion trap/time-of-flight mass spectrometer. *Rev. Sci. Instrum.* **70**: 4192–9.

Gaie-Levrel F, Garcia GA, Schwell M, Nahon L. 2011. VUV state-selected photoionization of thermally-desorbed biomolecules by coupling an aerosol source to an imaging photoelectron/photoion coincidence spectrometer: case of the amino acids tryptophan and phenylalanine. *Phys Chem. Chem. Phys.* **13**: 7024–36.

Gharaibeh MF, Bizau JM, Cubaynes D, Guilbaud S, Hassan NE, Shorman AI MM, Miron C, Nicolas C, Robert E, Blancard C, McLaughlin BM. 2011. K-shell photoionization of singly ionized atomic nitrogen: experiment and theory. *J. Phys. B: At., Mol. Opt. Phys.* **44**: 175208.

Gimonkinsel M, Kinsel G, Edmondson R, Russell D. 1995. Photodissociation of High Molecular Weight Peptides and Proteins in a Two-Stage Linear Time-Of-Flight Mass Spectrometer. *J. Chem. Phys.* **6**: 578–87.

Gindensperger E, Haegy A, Daniel C, Marquardt R. 2010 Ab initio study of the electronic singlet excited-state properties of tryptophan in the gas phase: The role of alanyl side-chain conformations. *Chem. Phys.* **374** : 104–10

Giuliani A, Milosavljević A R, Hinsén K, Canon F, Nicolas C, Réfrégiers M, Nahon L. 2012. Structure and charge-state dependence of gas phase ionization energy of proteins. *Angew. Chem., Int. Ed.* **51**: 9552–9556.

Gonzalez-Magaña O, Reitsma G, Bari S, Hoekstra R, Schlathölter T. 2012. Length effects in VUV photofragmentation of protonated peptides. *Phys. Chem. Chem. Phys.* **14**: 4351.

Gonzalez-Magaña O, Reitsma G, Tiemens M, Boschman L, Hoekstra R, Schlathölter T. 2012. Near-Edge X-ray Absorption Mass Spectrometry of a Gas-Phase Peptide. *J. Phys. Chem. A* **116**:10745–51

Gorman GS, Amster IJ. 1993. Photodissociation Studies of Small Peptide Ions by Fourier-Transform Mass-Spectrometry. *Org. Mass Spectrom.* **28**: 437–44.

Grégoire G, Jouvét C, Dedonder C, Sobolewski A L. 2007 Ab initio Study of the Excited-State Deactivation Pathways of Protonated Tryptophan and Tyrosine. *J. Am. Chem. Soc* **129** : 6223–31

Grégoire G, Lucas B, Barat M, Fayeton J, Dedonder-Lardeux C, Jouvét C. 2009 UV photoinduced dynamics in protonated aromatic amino acid. *Eur. Phys. J. D.* **51** : 109–16

Guan Z, Kelleher N, O'Connor P, Aaserud D, Little D, McLafferty F. 1996. 193 nm photodissociation of larger multiply-charged biomolecules. *Int. J. Mass Spectrom. Ion Processes.* **157**: 357–64.

Hatano Y. 1999. Interaction of vacuum ultraviolet photons with molecules. Formation and dissociation dynamics of molecular superexcited states. *Phys. Rep.* **313**: 109–69.

Helliwell JR. 1998. Synchrotron radiation facilities. *Nat. Struct. Biol.* **5**: 614–7.

Hinojosa G, Covington A, Phaneuf R, Sant'Anna M, Hernandez R, Covington I, Domínguez I, Bozek J, Schlachter A, Álvarez I, Cisneros C. 2002. Formation of long-lived CO₂⁺ via photoionization of CO⁺. *Phys. Rev. A.* **66**: 032718.

- Hirsch K, Lau J, Klar P, Langenberg A, Probst J, Rittmann J, Vogel M, Zamudio-Bayer V, Möller T, Issendorff B. 2009. X-ray spectroscopy on size-selected clusters in an ion trap: from the molecular limit to bulk properties. *J. Phys. B: At., Mol. Opt. Phys.* **42**: 154029.
- Hirsch K, Zamudio-Bayer V, Ameseder F, Langenberg A, Rittmann J, Vogel M, Möller T, Issendorff von B, Lau J. 2012. 2p x-ray absorption of free transition-metal cations across the 3d transition elements: Calcium through copper. *Phys. Rev. A.* **85**: 062501.
- Hunt DF, Shabanowitz J, Yates J R, Griffin P R And Zhu N Z 1989 Tandem Quadrupole Fourier-Transform Mass-Spectrometry *Anal. Chim. Acta.* **225**: 1–10.
- Ice GE, Budai J D, Pang JW. 2011. The Race to X-ray Microbeam and Nanobeam Science. *Science.* **334**: 1234–9
- Joly L, Antoine R, Allouche AR, Broyer M, Lemoine J, Dugourd P. 2007. Ultraviolet Spectroscopy of Peptide and Protein Polyanions in Vacuo: Signature of the Ionization State of Tyrosine. *J. Am. Chem. Soc.* **129**: 8428–9.
- Joly L, Antoine R, Broyer M, Lemoine J, Dugourd P. 2008. Electron Photodetachment from Gas Phase Peptide Dianions. Relation with Optical Absorption Properties. *J Phys Chem A.* **112**: 898–903.
- Kalcic CL, Reid GE, Lozovoy VV, Dantus M. 2012. Mechanism Elucidation for Nonstochastic Femto second Laser-Induced Ionization/Dissociation: From Amino Acids to Peptides. *J Phys Chem A.* **116**: 2764–74.
- Kalcic C, Gunaratne T, Jones A, Dantus M, Reid G. 2009. Femtosecond Laser-Induced Ionization/Dissociation of Protonated Peptides *J. Am. Chem. Soc.* **131**: 940–2.
- Kamatari Y O, Konno T, Kataoka M, Akasaka K. 1996. The methanol-induced globular and expanded denatured states of cytochrome c: A study by CD fluorescence, NMR and small-angle X-ray scattering. *J. Mol. Biol.* **259**: 512–23.
- Kelly S M, Jess TJ, Price NC. 2005. How to study proteins by circular dichroism. *Biochim. Biophys. Acta, Proteins Proteomics.* **1751**: 119–39.
- Khoury J T, Rodriguez-Cruz S E, Parks JH. 2002. Pulsed fluorescence measurements of trapped molecular ions with zero background detection. *J. Am. Soc. Mass Spectrom.* **13**: 696–708.
- Kilcoyne A, Aguilar A, Müller A, Schippers S, Cisneros C, Alna'Washi G, Aryal N, Baral K, Esteves D, Thomas C, Phaneuf R. 2010. Confinement Resonances in Photoionization of Xe@C60+. *Phys. Rev.Lett.* **105**: 213001.
- Kim TY, Schwartz JC, Reilly JP. 2009. Development of a Linear Ion Trap/Orthogonal-Time-of-Flight Mass Spectrometer for Time-Dependent Observation of Product Ions by Ultraviolet Photodissociation of Peptide Ions. *Anal. Chem.* **81**: 8809–17.
- Kjeldsen H. 2006. Photoionization cross sections of atomic ions from merged-beam experiments. *J. Phys. B: At., Mol. Opt. Phys.* **39**: R325–77.
- Kravis S, Church D, Johnson B, Meron M, Jones K, Levin J, Sellin I, Azuma Y, Mansour N and Berry H 1991 Inner-shell photoionization of stored positive ions using synchrotron radiation. *Phys. Rev. Lett.* **66**: 2956–9.
- Laskin J, Yang Z, Lam C, Chu I. 2007. Charge-remote fragmentation of odd-electron peptide ions. *Anal. Chem.* **79**: 6607–14.
- Lebrilla CB, Wang D, Mizoguchi TJ, Mciver RT. 1989. Comparison of the Fragmentation Produced by Fast Atom Bombardment and Photodissociation of Peptides. *J. Am. Chem. Soc.* **111**: 8593–8.

Lemaire J, Boissel P, Heninger M, Mauclaire G, Bellec G, Mestdagh H, Simon A, Le Caer S, Ortega J, Glotin F, Maitre P. 2002. Gas Phase Infrared Spectroscopy of Selectively Prepared Ions. *Phys. Rev. Lett.* **89**: 273002.

Lepere V, Lucas B, Barat M, Fayeton J A, Picard V J, Jouvet C, Çarçabal P, Nielsen I, Dedonder-Lardeux C, Grégoire G, Fujii A. 2007b Comprehensive characterization of the photodissociation pathways of protonated tryptophan. *J. Chem. Phys.* **127** : 134313

Lucas B, Barat M, Fayeton J A, Pérot M, Jouvet C, Grégoire G, Brøndsted Nielsen S. 2008 Mechanisms of photoinduced C α -C β bond breakage in protonated aromatic amino acids. *J. Chem. Phys.* **128** : 164302

Lyon I, Peart B, West J, Dolder K. 1986 .Measurements of Absolute Cross-Sections for the Photoionization of Ba⁺ Ions *J. Phys. B: At., Mol. Opt. Phys.* **19**: 4137–47.

Madsen J A, Boutz D R & Brodbelt J S. 2010. Ultrafast Ultraviolet Photodissociation at 193 nm and its Applicability to Proteomic Workflows. *J. Proteome Res.* **9**: 4205–14

March RE. 2009. Quadrupole ion traps. *Mass Spectrom. Rev.* **28**: 961–89.

Marshall AG, Hendrickson CL, Jackson GS. 1998. Fourier transform ion cyclotron resonance mass spectrometry: A primer. *Mass Spectrom. Rev.* **17**: 1–35.

Martin S A, Hill J A, Kittrell C, Biemann K. 1990. Photon-induced dissociation with a four-sector tandem mass spectrometer. *J. Am. Soc. Mass Spectrom.* **1**: 107–9.

Mauclaire G, Lemaire J, Boissel P, Bellec G, Heninger M. 2004. MICRA: a compact permanent magnet Fourier transform ion cyclotron resonance mass spectrometer *Eur. J. Mass Spectrom.* **10**: 155–62.

McCullough BJ, Entwistle A, Konishi I, Buffey S, Hasnain SS, Brancia FL, Grossmann J G, Gaskell SJ. 2009 Digital Ion Trap Mass Spectrometer for Probing the Structure of Biological Macromolecules by Gas Phase X-ray Scattering. *Anal. Chem.* **81**: 3392–7.

McLafferty FW. 1980. Tandem mass spectrometry (MS/MS): a promising new analytical technique for specific component determination in complex mixtures. *Accounts Chem. Res.* **13**: 33–9.

Milosavljević AR, Nicolas C, Lemaire J, Dehon C, Thissen R, Bizau JM, Réfrégiers M, Nahon L, Giuliani A. 2011. Photoionization of a protein isolated in vacuo. *Phys. Chem. Chem. Phys.* **13** : 15432–6.

Milosavljević AR, Canon F, Nicolas C, Miron C, Nahon L, Giuliani A. 2012a. Gas-Phase Protein Inner-Shell Spectroscopy by Coupling an Ion Trap with a Soft X-ray Beamline. *J. Phys. Chem. Lett.* **3**: 1191–6.

Milosavljević AR, Nicolas C, Gil JF, Canon F, Refregiers M, Nahon L, Giuliani A. 2012b. Fast in vacuo photon shutter for synchrotron radiation quadrupole ion trap tandem mass spectrometry. *Nucl. Instrum. Methods Phys. Res., Sect. B.* **279**: 34–6.

Milosavljević A R, Nicolas C, Gil J-F, Canon F, Réfrégiers M, Nahon L, Giuliani A 2012c VUV synchrotron radiation: a new activation technique for tandem mass spectrometry. *J. Synchrotron Rad.* **19**: 174–8.

Moon J H, Yoon SH, Kim MS. 2005. Photodissociation of singly protonated peptides at 193 nm investigated with tandem time-of-flight mass spectrometry. *Rapid Commun. Mass Spectrom.* **19**: 3248

Nahon L, de Oliveira N, Garcia GA, Gil J-F, Pilette B, Marcouille O, Lagarde B, Polack F. 2012. DESIRS: a state-of-the-art VUV beamline featuring high resolution and variable polarization for spectroscopy and dichroism at SOLEIL. *J. Synchrotron Rad.* **19**: 508-520.

Nagornova NS, Rizzo TR, Boyarkin OV. 2012. Interplay of Intra- and Intermolecular H-Bonding in a Progressively Solvated Macrocyclic Peptide. *Science.* **336** : 320–3.

- Niemeyer M, Hirsch K, Zamudio-Bayer V, Langenberg A, Vogel M, Kossick M, Ebrecht C, Egashira K, Terasaki A, Möller T, Issendorff von B, Lau J. 2012. Spin Coupling and Orbital Angular Momentum Quenching in Free Iron Clusters. *Phys. Rev. Lett.* **108**: 057201.
- Oh J, Moon J, Kim M. 2005. Chromophore effect in photodissociation at 266 nm of protonated peptides generated by matrix-assisted laser desorption ionization (MALDI). *J. Mass Spectrom.* **40**: 899–907.
- Oomens J, van Roij AJA, Meijer G, von Helden G. 2000. Gas-Phase Infrared Photodissociation Spectroscopy of Cationic Polyaromatic Hydrocarbons. *ASTROPHYS J.* **542**: 404–10.
- Parthasarathi R, He Y, Reilly JP, Raghavachari K. 2010. New Insights into the Vacuum UV Photodissociation of Peptides. *J. Am. Chem. Soc.* **132**: 1606–10.
- Peart B, Stevenson JG, Dolder KT. 1973. Measurements of Cross-Sections for Ionization of Ba⁺ by Energy Resolved Electrons. *J. Phys. B: At., Mol. Opt. Phys.***6**: 146–9.
- Pérot M, Lucas B, Barat M, Fayeton J A, Jouvét C. 2010 Mechanisms of UV Photodissociation of Small Protonated Peptides. *J Phys Chem A* **114** : 3147–56
- Perry RH, Cooks RG Noll RJ. 2008. Orbitrap mass spectrometry: instrumentation, ion motion and applications. *Mass Spectrom. Rev.***27**: 661–99.
- Piancastelli M N, Simon M and Ueda K 2010 Present trends and future perspectives for atomic and molecular physics at the new X-ray light sources *J. Electron. Spectrosc. Relat. Phenom.* **181**: 98–110.
- Reilly JP. 2009. Ultraviolet photofragmentation of biomolecular ions. *Mass Spectrom. Rev.* **28**: 425–47.
- Rizzo TR, Stearns JA, Boyarkin OV. 2009. Spectroscopic studies of cold, gas-phase biomolecular ions. *Int. Rev. Phys. Chem.* **28**: 481–515.
- Robin MB. 1975. Higher excited states of polyatomic molecules. Volume I. New York : Academic Press. p.76.
- Schwartz JC, Senko MW, Syka JEP. 2002. A two-dimensional quadrupole ion trap mass spectrometer. *J. Am. Soc. Mass. Spectrom.* **13**: 659–69.
- Scully S, Emmons E, Gharaibeh M, Phaneuf R, Kilcoyne A, Schlachter A, Schippers S, Müller A, Chakraborty H, Madjet M, Rost J. 2007. Scully et al., Reply. *Phys. Rev. Lett.* **98**: 179602.
- Serrano-Andrés L, Roos B O 1996 a. Theoretical study of the absorption and emission spectra of indole in the gas phase and in a solvent *J. Am. Chem. Soc.* **118** : 185–95
- SerranoAndres L, Fülischer M. 1996 b. Theoretical study of the electronic spectroscopy of peptides .2. Glycine and N-acetyl glycine. *J. Am. Chem. Soc.* **118**: 12200–6
- Serrano-Andrés L, Fülischer MP. 1998. Theoretical Study of the Electronic Spectroscopy of Peptides. III. Charge-Transfer Transitions in Polypeptides *J. Am. Chem. Soc.* **120**: 10912–20.
- Serrano-Andrés L, Fülischer MP. 2001. Charge Transfer Transitions in Neutral and Ionic Polypeptides: A Theoretical Study *J. Phys. Chem. B.* **105**: 9323–30.
- Shelimov K, Clemmer D, Hudgins R, Jarrold M. 1997. Protein structure in vacuo: Gas-phase confirmations of BPTI and cytochrome c. *J. Am. Chem. Soc.* **119**: 2240–8.
- Shvartsburg AA, Li F, Tang K, Smith RD. 2006. Characterizing the structures and folding of free proteins using 2-D gas-phase separations: observation of multiple unfolded conformers. *Anal Chem.* **78**: 3304–15.

Simon M, CrespoLópez-Urrutia J, Beilmann C, Schwarz M, Harman Z, Epp S, Schmitt B, Baumann T, Behar E, Bernitt S, Follath R, Ginzel R, Keitel C, Klawitter R, Kubiček K, Mäckel V, Mokler P, Reichardt G, Schwarzkopf O, Ullrich J. 2010 Resonant and Near-Threshold Photoionization Cross Sections of Fe¹⁴⁺. *Phys. Rev. Lett.* **105**: 183001.

Stewart-Ornstein J, Hitchcock AP, Hernández Cruz D, Henklein P, Overhage J, Hilpert K, Hale JD, Hancock REW. 2007. Using Intrinsic X-ray Absorption Spectral Differences To Identify and Map Peptides and Proteins. *J. Phys. Chem. B.* **111**: 7691–9.

Tabarin T, Antoine R, Broyer M, Dugourd P. 2005. Specific photodissociation of peptides with multi-stage mass spectrometry. *Rapid Commun. Mass Spectrom.* **19** : 2883–92

Thelen JJ, Miernyk JA. 2012. The proteomic future: where mass spectrometry should be taking us. *Biochem. J.* **444**: 169–81.

Thissen R, Bizau J M, Blancard C, Coreno M, Dehon C, Franceschi P, Giuliani A, Lemaire J, Nicolas C. 2008. Photoionization cross section of Xe⁺ ion in the pure 5p⁵ 2P_{3/2} ground level. *Phys. Rev. Lett.* **100**: 223001.

Thompson M, Cui W, Reilly J. 2007. Factors that impact the vacuum ultraviolet photofragmentation of peptide ions *J. Am. Soc. Mass. Spectrom.* **18**: 1439–52.

Thompson M, Cui W, Reilly J. 2004. Fragmentation of singly charged peptide ions by photodissociation at $\lambda = 157$ nm. *Angew. Chem. Int. Ed.* **43**: 4791–4.

Valentine SJ, Counterman AE, Clemmer DE. 1997. Conformer-dependent proton-transfer reactions of ubiquitin ions. *J. Am. Soc. Mass. Spectrom.* **8**: 954–61.

Vogel M, Kasigkeit C, Hirsch K, Langenberg A, Rittmann J, Zamudio-Bayer V, Kulesza A, Mitrić R, Möller T, von Issendorff B, Lau J. 2012. 2p core-level binding energies of size-selected free silicon clusters: Chemical shifts and cluster structure. *Phys. Rev. B.* **85**: 195454.

Wang LS, Wang XB. 2000. Probing Free Multiply Charged Anions Using Photodetachment Photoelectron Spectroscopy. *J Phys Chem A.* **104**: 1978–90.

West J. 2001. Photoionization of atomic ions. *J. Phys. B: At., Mol. Opt. Phys.* **34**: R45–R91.

Williams ER, McLafferty FW. 1990. 193 nm Laser photoionization and photodissociation for isomer differentiation in Fourier-transform mass spectrometry. *J. Am. Soc. Mass. Spectrom.* **1**: 361–5.

Williams ER, Furlong JJP, McLafferty FW. 1990. Efficiency of collisionally-activated dissociation and 193-nm photodissociation of peptide ions in fourier transform mass spectrometry. *J. Am. Soc. Mass. Spectrom.* **1**: 288–94.

Zhang L and Reilly J P. 2009. Radical-driven dissociation of odd-electron peptide radical ions produced in 157 nm photodissociation. *J. Am. Soc. Mass Spectrom.* **20**: 1378–90

Zubarev R A & Yang H. 2010. Multiple Soft Ionization of Gas-Phase Proteins and Swift Backbone Dissociation in Collisions with ≤ 99 eV Electrons. *Angew. Chem. Int. Ed.* **49**: 1439 –1441